

CHALMERS



Coupling between changes in hydraulic and mechanical aperture

A laboratory study on rock cores

JOHAN THÖRN

Department of Civil and Environmental Engineering
Division of GeoEngineering
Engineering Geology Research Group
CHALMERS UNIVERSITY OF TECHNOLOGY
Gothenburg, Sweden 2012
Report 2012:9

Report 2012:9

Coupling between changes in hydraulic
and mechanical aperture

A laboratory study on rock cores

Johan Thörn

Department of Civil and Environmental Engineering
Division of GeoEngineering
Engineering Geology Research Group
Chalmers University of Technology

Gothenburg, Sweden 2012

Coupling between changes in hydraulic and mechanical aperture

A laboratory study on rock cores

Johan Thörn

© JOHAN THÖRN, 2012

Report / Department of Civil and Environmental Engineering, Chalmers University of Technology 2012:9. ISSN-1652-9162

Department of Civil and Environmental Engineering

Division of GeoEngineering

Engineering Geology Research Group

Chalmers University of Technology

SE-412 96 Gothenburg

Sweden

Telephone: + 46 (0)31-772 1000

Cover:

The permeameter cell that was used for the experiments.

Chalmers Reproservice

Gothenburg, Sweden 2012

Contents

CONTENTS	I
PREFACE	II
1 BACKGROUND	1
2 EQUIPMENT	3
2.1 Sample preparation and mounting	3
2.2 De-aeration	5
2.3 Flow measurement	5
2.4 Testing of equipment	6
2.4.1 Tightness	6
2.4.2 Laminar or turbulent flow	6
2.5 Sensors	7
2.5.1 Displacement gauge	7
2.5.2 Pore pressure sensor	7
3 EXPERIMENTS	8
3.1 Experimental procedure	8
3.1.1 Confining pressure sequence	8
3.1.2 Data collection	9
3.2 Validity and sensitivity of test conditions	9
4 RESULTS	11
5 REFERENCES	12
APPENDIX I. TEST PROTOCOL FLOW TEST	13
APPENDIX II. PHOTOS OF EQUIPMENT	15
APPENDIX III. TEST PROTOCOLS FROM EXPERIMENTS	17
APPENDIX IV. FRACTURE TRACES	23
APPENDIX V. PHOTOS OF SAMPLES	25
APPENDIX VI. ANALYSIS SHEET PS0039061	33
APPENDIX VII. ANALYSIS SHEET AB1AB2	41
APPENDIX VIII. ANALYSIS SHEET PS0037053	51
APPENDIX IX. ANALYSIS SHEET PS0039023	61
APPENDIX X. INFLUENCE OF THE COMPRESSIBILITY OF WATER	71
APPENDIX XI. NOTE ON UNCERTAINTIES	73

Preface

This laboratory experiment series was conducted by Johan Thörn, in spring 2011 as a part of the PhD-project *Hydromechanical Properties of Fractures and Fracture Zones*, and more specific to contribute to research-goals, such as:

- Analysing and predicting fracture stiffness and hydraulic aperture development in granitic rock.
- Increasing understanding of how real fracture aperture and hydraulic aperture and contact point distributions affect scale properties in situ and in lab.
- Increasing understanding of how parameters, measurable in situ and in lab can be used to characterize fracture stiffness.

Great help with building, setting up and adjusting the equipment was provided by Aaro Pirhonen and Peter Hedborg. Supervision, support and feedback were provided by Åsa Fransson, Lars O Ericsson and Gunnar Gustafson as well as practical advice from Petra Brinkhoff.

This report is a summary of the results and presents the experimental setup, measurement values and pictures on equipment and samples and is intended as a background reference for a journal article where the space for such details is more limited.

Gothenburg, December 2012

Johan Thörn

1 Background

This section briefly describes the equations that are used for evaluating and analyzing the results.

Flow of water is somewhat trivially calculated as volume per time:

$$Q = \frac{V}{t} \quad (1)$$

Transmissivity, T is in analogy with Darcy's law expressed as (2) (Gustafson 2012) Where the length, L and width, W of the fracture is measured for each sample.

$$T = \frac{Q \cdot L}{dh \cdot W} \quad (2)$$

With transmissivity known, the cubic law, (3) can be used for calculating the hydraulic aperture, b . This expression also requires values of viscosity and weight of water, which is found in standard tables if the water temperature is known.

$$b = \sqrt[3]{\frac{12 \cdot \mu_w \cdot T}{\rho_w \cdot g}} \quad (3)$$

The relation between fracture normal stiffness and storativity used by Doe and Geier (1990), was combined with the relation between storativity and transmissivity, presented by Rhén et al. (2008), by Fransson (2009), under the assumption that the compressibility of water is negligible, rendering (4), and (5). Now we are at a fracture normal stiffness derived from time, volume and temperature of the water flow through a sample (5).

$$k_n^S = \frac{\rho_w \cdot g}{S} \quad (4)$$

$$k_n^S = \frac{\rho_w \cdot g}{0.0109 \cdot T^{0.71}} \quad (5)$$

Fracture normal stiffness can also be estimated as aperture change per normal stress change, which is used in (6) and (7), where p is the cell pressure, represented as p_1 and p_2 , i.e. the pressure before and after a stepwise change to cell pressure. This is acting as normal stress change. Δa is measured physical deformation, and b is hydraulic aperture according to (3).

$$k_n^a = \frac{p_2 - p_1}{\Delta a} \quad (6)$$

$$k_n^b = \frac{p_2 - p_1}{b_2 - b_1} \quad (7)$$

2 Equipment

The permeameter itself consists of a stainless steel cell where an isotropic pressure can be set up to 2.5 MPa, Figure 1. For security the cell is filled with water, and pressurized with a small volume of compressed air. The cell water is colored, enabling detection of leakage into the sample. The tested fracture is ideally vertical in the center of the sample, and water is led into the sample from below, and distributed across the bottom area by a milled depression with a steel mesh. The same type of mesh is used in the lid for collecting the sample water to the pipe that protrudes out of the cell. A deformation sensor is mounted in plastic brackets, which are glued to the sample. The sensor and brackets are housed in a milled hole in the lid. See schematic representation in Figure 1.

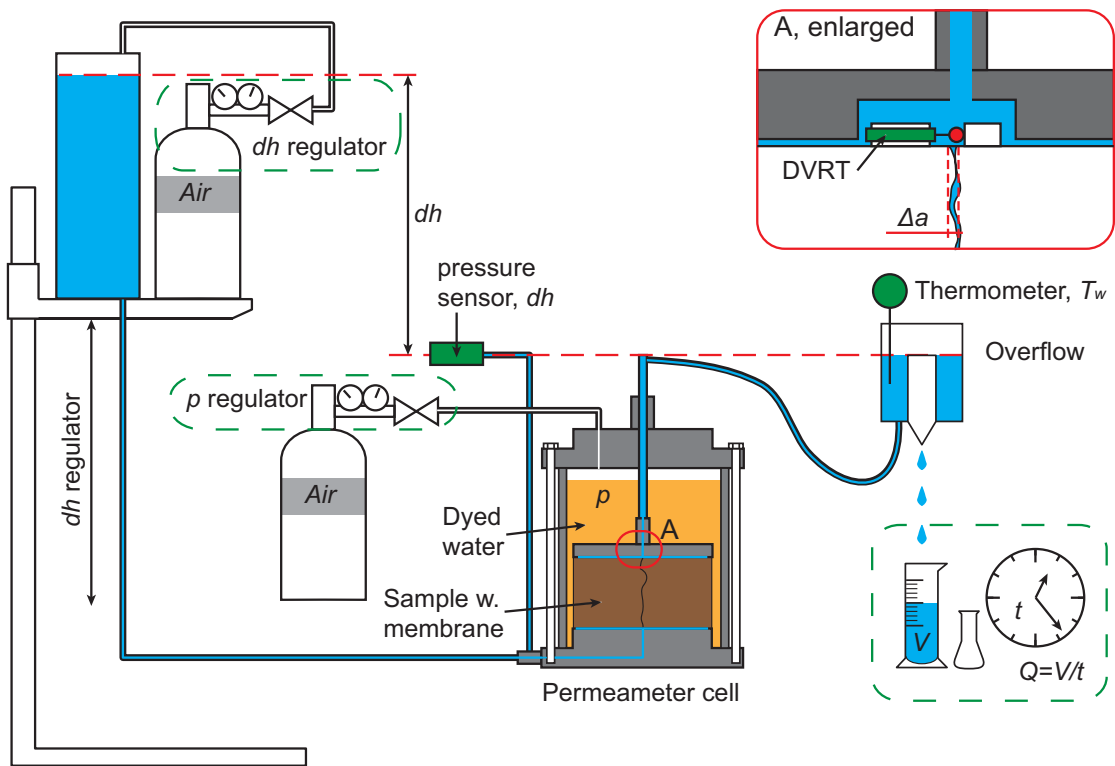


Figure 1: Schematic representation of test setup, and measured parameters. Measurements are marked with green; where digital logging is filled green, and manual monitoring and measurement have dashed green frames. Water is blue, colored water is orange and compressed air is grey. The bulk part of dh is set by compressed air, while fine adjustments are made by elevating the water container, with instant feedback from pressure sensor, dh .

2.1 Sample preparation and mounting

Ericsson et al. (2009) used samples that were core drilled from slabs taken from the walls of TASS and TASQ tunnels in Äspö HRL. While drilling samples from slabs steel plates were bolted across the fracture, holding the parts together. The cores are stored with rubber-bands holding the halves in place. In the experiments described here the cores from Ericsson et al. (2009) were reused. For mounting in the cell, the core is placed on the steel bottom and two latex-rubber membranes are carefully

applied by means of vacuum sucking the membrane to the inside of a pipe, and releasing the membrane when in place. The ends are folded, giving four layers of membrane. On the steel bottom and the steel top plate of the cell the membranes are tightened with rubber O-rings. A cutaway photo-montage of a mounted sample is found in Figure 3.



Figure 2: Membrane mounting on plastic sample-dummy

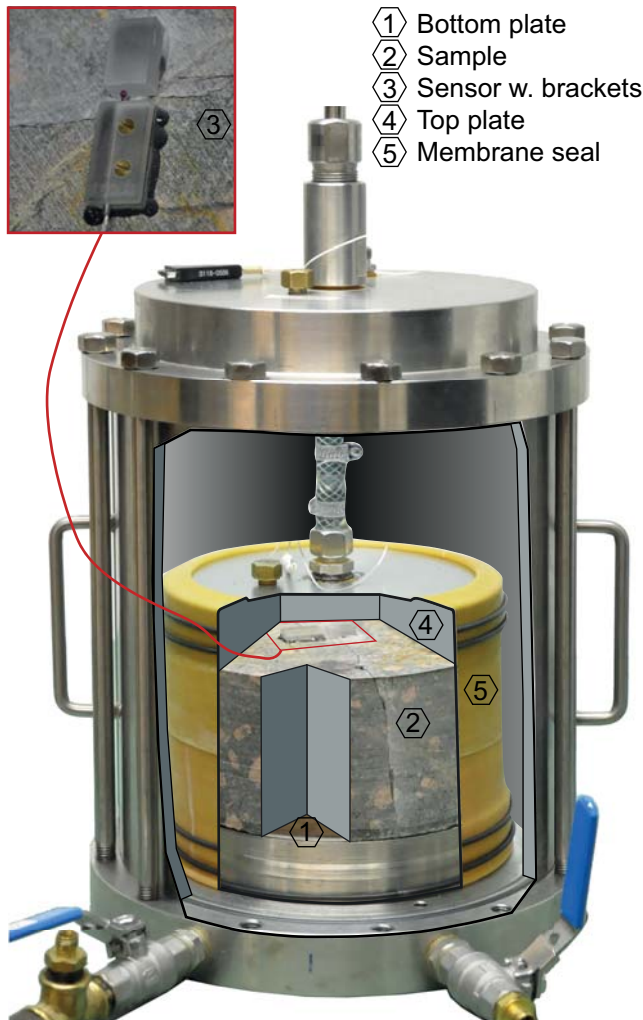


Figure 3: Cutaway photo-montage of a sample mounted in the cell.

2.2 De-aeration

The container for sample water houses about 18 l of water, and prior to testing the water is de-aerated by a vacuum pump, with an approximate pressure of - 0.9 bar (relative atmospheric pressure). This is done for at least 3 hours. The pump is able to deliver 20 mBar total pressure, but this might not be fully achieved in the fairly large system during the three hours of pumping. The sample is filled with the de-aerated water, and air is sucked out of the sample with the same pump.

2.3 Flow measurement

The flow through the system is led out of the cell in a pipe and series of hoses is connected to that pipe. For high flow samples the water is led into a container of approximately 1 l, where it overflows into a hose down to a graded measurement glass (100 ml, 50 ml, 20 ml) or Erlenmeyer flask (10 ml, 2 ml) (see sketch in Figure 1). The overflowing surface gives a steady flow, which easily can be measured and timed. The overflowing surface also allows easy measurement of the sample water pressure loss, dh . The overflow surface and the pressure sensor is placed on the same height;

therefore the sensor show the pressure loss across the sample. For low flow samples (T approximately less than $10^{-8} \text{ m}^3/\text{s}$), dh is set higher, and the water is led directly to a small piece of hose that is put directly on the out-pipe from the cell, the surface in the hose is marked, and afterwards the volume between the markings is weighed (as for the tightness testing, described in section 2.4.1 below). The flow is calculated according to equation (1) which is used in equation (2) to evaluate a transmissivity that is used in equation (3) to calculate a cubic-law hydraulic aperture.

2.4 Testing of equipment

2.4.1 Tightness

The tightness of the setup was tested with a plastic sample-dummy, a cell confining pressure of 2 MPa, and sample pressure of 0.25 MPa. During one hour 0.3g water got through the system, corresponding to a transmissivity of less than $1.5 \times 10^{-12} \text{ m}^2/\text{s}$. For tests with flow rates corresponding to $T > 10^{-9} \text{ m}^2/\text{s}$ this potential leakage can be neglected.

2.4.2 Laminar or turbulent flow

A core sample (PS0039061) with an aperture of approximately 100 μm was tested if the flow through the fracture was likely to be laminar or turbulent. A confining pressure of 0.5 MPa and dh from 0.7 to 5 m was used. Reynolds number was calculated according to (8), and resulted in values spanning from 6 to 40; all indicating laminar flow (less than 2000). The flow in the hose and pipe out of the sample had Reynolds numbers up to 500; also laminar. Losses due to friction of the flow in pipes, and flow in and out of the hose results in pressure losses of 1 to 7 mm pressure head. For the actual testing $dh = 0.64 \text{ m}$ was used for fractures with apertures down to approximately $b = 40 \mu\text{m}$, and $dh = 35.1 \text{ m}$ for apertures less than 40 μm . A plot of hydraulic gradient against hydraulic aperture is used by (Gustafson 2012) for illustrating the transitions from laminar to turbulent flow for rough fracture surfaces, as well as smooth parallel plates, see Figure 4. The gradients of the experiments described here, as well as the samples from TASS tunnel described in (Ericsson et al. 2009) are shown in Figure 4.

$$R_e = \frac{\rho v D_f}{\mu} \quad (8)$$

Where

ρ is the density of water

v is the velocity of flow

D_f is the hydraulic diameter, defined as 4 times fracture cross-section area divided by circumference of the same area, and

μ is the viscosity of water

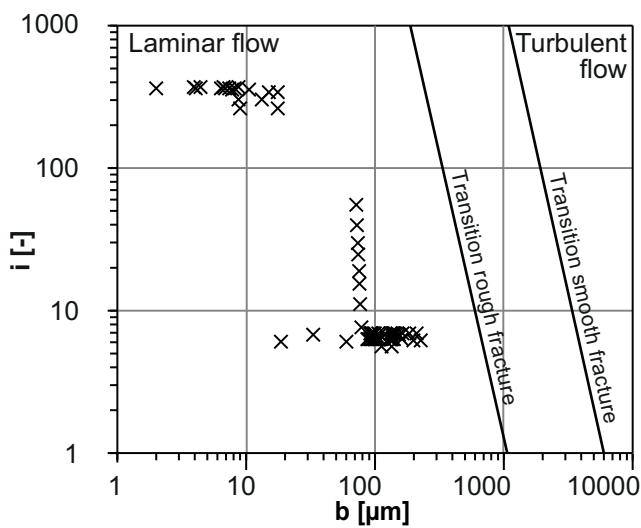


Figure 4: Hydraulic gradient and hydraulic aperture for samples in relation to the transition from laminar to turbulent flow.

2.5 Sensors

2.5.1 Displacement gauge

A Microstrain DVRT® with a stroke of 3 mm and resolution of 1.5 μm was used for deformation measurements across fractures. Calibration was performed with thickness gauges of 0.1 and 0.15 mm when the sensor was mounted.

2.5.2 Pore pressure sensor

Water with a specific pressure head, dh , was applied to the core from beneath (see Figure 1). The pressure was set by applying an air pressure to the surface of the water container. The pressure was fine-tuned by elevating the water container. Just before entering the cell (upstream) a hose to a pressure sensor was connected. The pressure sensor was set on the same height as the highest level of the water on the outside of the downstream-side of the cell; the overflow where water flows to a graded container for flow measurement. For low pressure tests a sensor calibrated for 0-5 meters of water column was used, and for higher pressure one calibrated for 0-35 meters of water column.

3 Experiments

3.1 Experimental procedure

The procedure for conducting the hydromechanically coupled experiments is summarized in the list below.

1. Plastic brackets were glued to the core halves
 2. The deformation sensor was installed in the plastic brackets and calibrated at 0.1 and 0.15 mm
 3. The sample was sealed with latex rubber membranes in the permeameter
 4. The cell was filled with dyed water and closed
 5. De-gassing of water container and saturation of sample were carried out through vacuum-suction of the test apparatus and sample during 3h
 6. Air temperature was measured
 7. Logging of dh and deformation were started
 8. Initial confining pressure was applied
 9. The valves were opened, to initiate the flow through the sample
 10. The initial deformation was given some time to stabilize
 11. Flow test in four load cycles was carried out while monitoring the temperature change in the outflow container
- For each pressure step:
- a. Time for start of pressure adjustment was noted
 - b. Time when the pressure adjustment was finished was noted
 - c. Three volume-time measurements of the flow were carried out during 10-30 min, preferably 15-20 minutes.

3.1.1 Confining pressure sequence

The hydromechanical testing utilized multiple pressure steps in four load cycles, see Figure 5. The time span for each step was chosen as a tradeoff between achieving perfectly stable values, and managing an entire test during a day. Test times were adjusted by varying the size of the container to fill. The following two conditions were applied:

- a. Sufficient time for three similar flow readings of a volume taking 1-5 minutes to fill: 100, 50, 20, 10 or 2 ml, depending on aperture.
- b. Sufficient time for achieving a stable reading on the deformation logger, about 10-30 minutes, preferably 15-20.

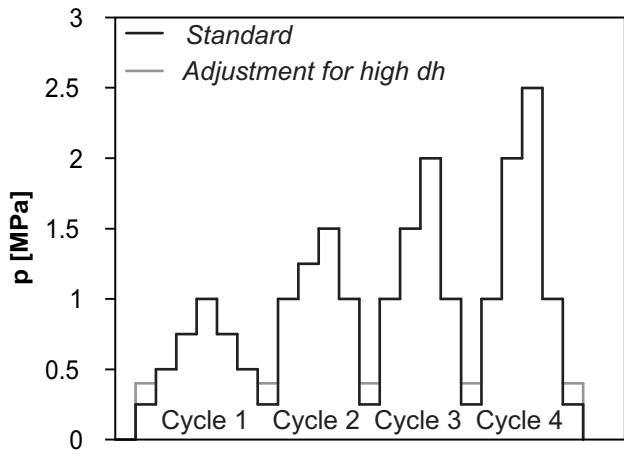


Figure 5: The pressure steps and cycles applied to the hydromechanical testing. The grey line represents an adjusted sequence that was used for samples with low transmissivity where dh was set to 0.351 MPa.

3.1.2 Data collection

The dh -pressure level was collected at one reading per second and plotted at a screen. The water storage container was raised accordingly, so that the water level, i.e. pressure head remained constant relative to the sample (see Figure 1). Deformation data was also collected at one reading per second and plotted at the screen. Flow volume was measured using graded measurement cylinders (100 ml, 50 ml and 20 ml) and Erlenmeyer flasks (10 ml and 2 ml). The corresponding time to fill was recorded using a time stamp macro in a Microsoft Excel-spreadsheet running on the same computer as the logging software for dh -pressure and Δa -deformation, which yielded a synchronized time value for all data sets.

3.2 Validity and sensitivity of test conditions

Larsson (1997) derived the pressure over a fracture through a biaxially loaded cylindrical rock sample to be a homogenous normal pressure equal to the cell pressure. This derivation is also valid for the case of three-dimensional hydrostatic loading, since the volumetric stress over the fracture is equal to the cell pressure. The effect of the water inside the fracture is insignificant, since this pressure is about 0.5 m water column. Iwano (1995), conducted triaxial testing of rock cores, and concluded that it did not seem to make a difference if the stress was applied as normal stress or confining stress. Therefore, the confining pressure step change is used as numerator in (6) and (7) i.e. normal stress change.

The chosen stress range for the experiments, 0-2.5 MPa was based on a basic distinct element analysis of the stresses in the area of the sawed-out slot using an idealized tunnel contour in Rocscience Examine 2D, but other than the exact blasted contour shape; real data (Ericsson et al. 2009). The three secondary stresses were all estimated to be within approximately 0-7 MPa in the rock volume of the slabs, where the samples were taken. An estimation with positions and orientations of the specific sampled fractures, still with an idealized tunnel contour, also resulted in normal and

shear stresses in the range of 0-8 MPa. For the hydromechanically tested samples the normal and shear stresses are; PS0037053 and PS0037061: 1-1.5 MPa, PS0039023: 4-8 MPa and PS0039061: 3-5 MPa.

At each pressure step the flow value was measured three times. With few exceptions, flow readings two and three were successively smaller than the first one or two readings for that confining pressure step. The value of the third reading was used for further analysis, supported by the fact that the flow seemed to asymptotically approach a stable value.

4 Results

In Figure 6 the results of flow expressed as hydraulic aperture, and mechanical deformation is shown. Values of the flow and deformation are presented in the appendices.

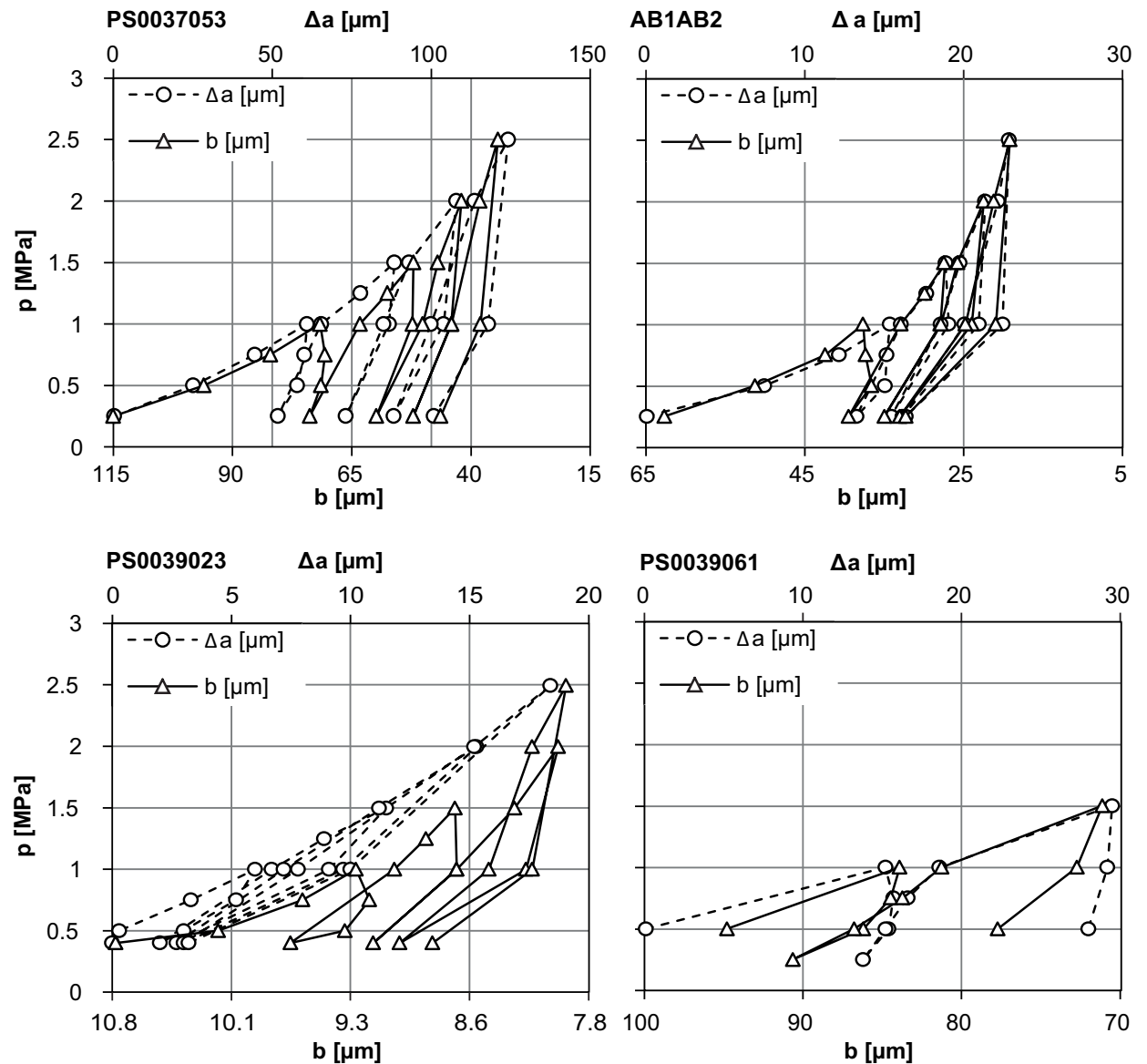


Figure 6: Sample PS0037053, PS0039023, AB1AB2 and PS0039061. Four load cycles with mechanical deformation, Δa , on the lower horizontal axis, and hydraulic aperture, b , on the upper horizontal axis. Note that the scales are different, with $\Delta b/\Delta a$ -ratios of 0.65, 0.15, 1.91 and 0.81.

5 References

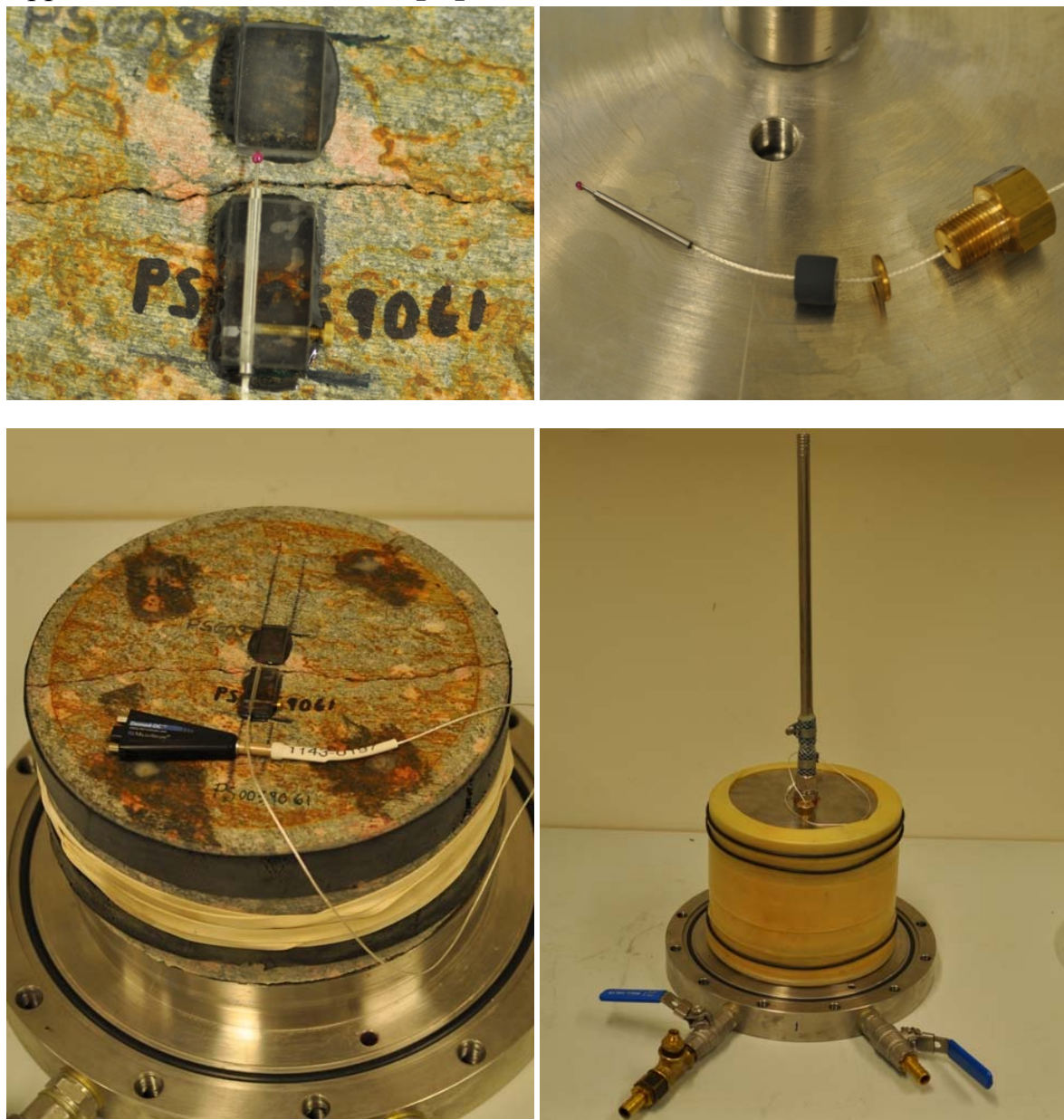
- Doe TW, Geier JE (1990) Interpretations of Fracture System Geometry Using Well Test Data, SKB Stripa Project TR 91-03. Swedish Nuclear Fuel and Waste Management Co, Stockholm, Sweden
- Ericsson LO, Brinkhoff P, Gustafson G, Kvartsberg S (2009) Hydraulic Features of the Excavation Disturbed Zone - Laboratory investigations of samples taken from the Q- and S-tunnels at Äspö HRL. R-09-45. Swedish Nuclear Fuel and Waste Management Co, Stockholm, Sweden
- Fransson Å (2009) Literature survey: Relations between stress change, deformation and transmissivity for fractures and deformation zones based on in situ investigations. R-09-13. Swedish Nuclear Fuel and Waste Management Co, Stockholm, Sweden
- Gustafson G (2012) Hydrogeology for Rock Engineers. BeFo, Stockholm, Sweden
- Iwano M (1995) Hydromechanical Characteristics of a Single Rock Joint. Massachusetts Institute of Technology,
- Larsson E (1997) Groundwater flow through a natural fracture -flow experiments and numerical modelling. Chalmers University of Technology, Gothenburg
- Rhén I, Forsmark T, Hartley L, Jackson P, Roberts D, Swan D, Gylling B (2008) Hydrogeological conceptualisation and parameterisation, Site descriptive modelling SDM–Site Laxemar. R-08-78. Swedish Nuclear Fuel and Waste Management Co, Stockholm, Sweden

Appendix I. Test protocol flow test

The protocol for flow tests is presented below. A click on the time stamp-button gives current time from the computer, same as logging of deformation and pressure data. The adjustment started and adjustment finished time stamps are used for drawing the cell-pressure graph. The difference between fill finished and fill started is calculated, and used in the analysis spreadsheet. The appearance of the analysis sheet can be seen in the appendices with individual results.

Protocol							Coupling between changes in hydraulic and mechanical aperture						
-Laboratory experiment							Johan Thörn, PhD student, Division of GeoEngineering, Chalmers University of Technology						
							Time stamp						
Pressure step (bar)	Adjustment started	Adjustment finished	Volume (ml)	Fill started	Fill finished	Fill time (s)	Notes						
2,5			100				0						
			100				0						
			100				0						
5			100				0						
			100				0						
			100				0						
			100				0						
7,5			100				0						
			100				0						
			100				0						
10			100				0						
			100				0						
			100				0						
			100				0						
7,5			100				0						
			100				0						
			100				0						
5			100				0						
			100				0						
			100				0						
2,5			100				0						
			100				0						
			100				0						

Appendix II. Photos of equipment

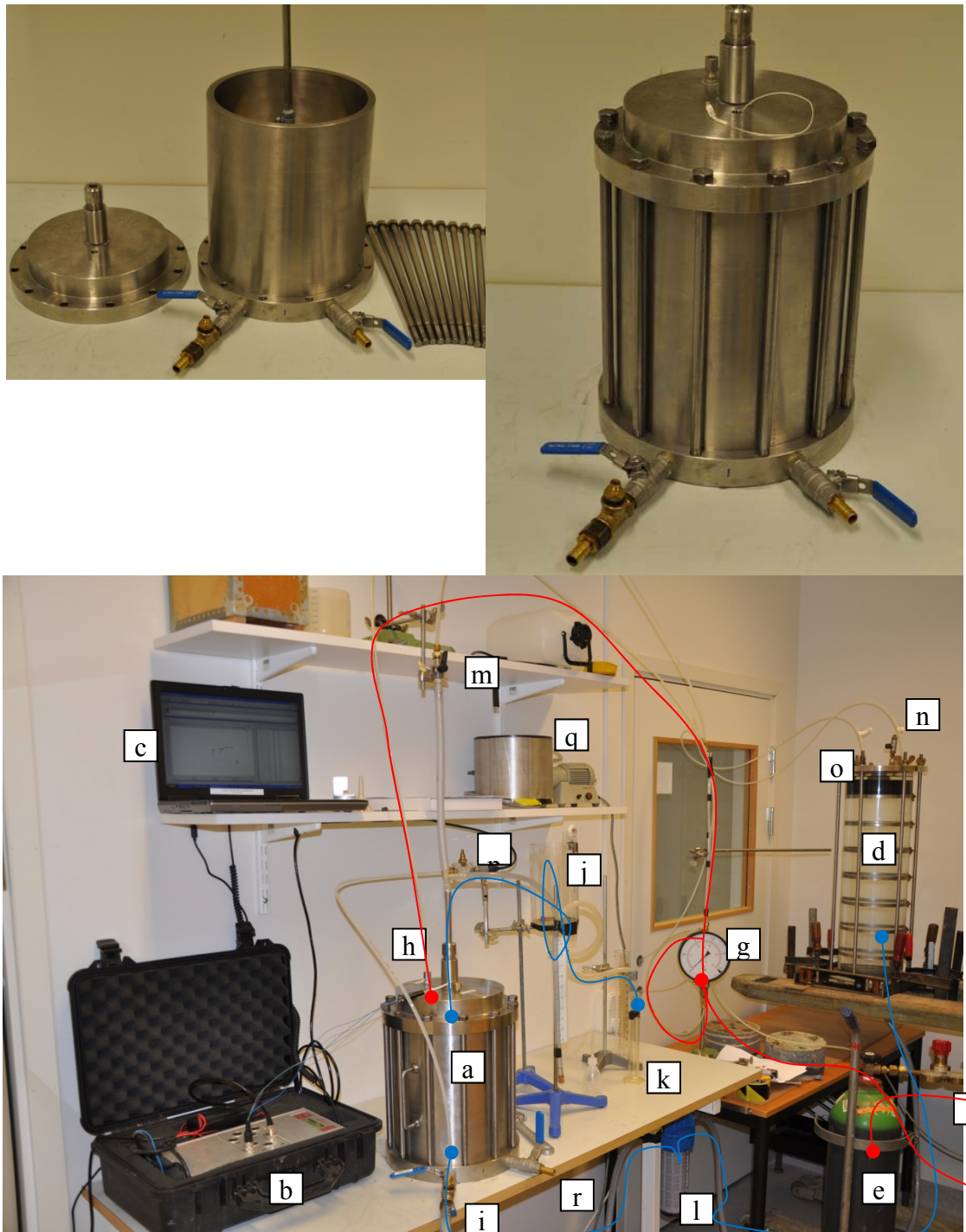


Top left: Sensor in plastic brackets. For the subsequent samples another type of bracket was used.

Top right: Sensor and the parts for getting it through the lid.

Lower left: Sensor on core sample

Lower right: Core mounted in latex rubber (the rubber in the left figure was removed before fitting this).



- a) Permeameter cell
- b) Data logger, dh and a
- c) Computer for real time data display
- d) Tank for water
- e) Compressed air for cell pressure, p
- f) Cell pressure regulator
- g) Cell pressure display
- h) Cell pressure inlet
- i) Water flow inlet
- j) Water flow outlet
- k) Water flow measurement, Q
- l) Filter for water
- m) Valve for degassing sample water
- n) Tank water degassing
- o) Compressed air inlet for dh
- p) Pressure sensor, dh
- q) Equipment for applying membranes
- r) Cell water dump valve
- Blue line, Q water path
- Red line, p cell pressure path

Appendix III. Test protocols from experiments

Calibration, test and practice runs:

1. Core PS0039061, validation of method, 2011-01-18.

Hydromechanical experiments

A table including pressure step adjustment times and flow measurement times is presented for each sample. Deformation and pressure data is presented in the analysis sheets (appendices).

1. Core AB1AB2, tested on 2011-02-15
2. Core PS0037053, tested on 2011-02-24
3. Core PS0039023, tested on 2011-03-01
4. (Core PS0039021) excluded due to the results of the other cores.

Cycle: 1 Core: AB1AB2							
Pressure							
step (bar)	Adjustment started	Adjustment finished	Volume (ml)	Fill started	Fill finished	Fill time (s)	Notes
2,5	10:11:17	10:12:29	100	10:24:18	10:30:35	377	
			100	10:31:17	10:38:01	404	
			100	10:38:37	10:45:34	417	
5	10:45:54	10:47:21	50	10:49:11	10:55:04	353	
			50	10:56:12	11:02:25	373	
			50	11:02:57	11:09:18	381	
7,5	11:10:31	11:11:34	50	11:14:48	11:25:04	616	
			50	11:25:39	11:36:24	645	
			50	11:36:46	11:47:58	672	
10	11:48:59	11:50:20	20	11:51:25	11:57:52	387	
			20	12:01:08	12:07:50	402	
			20	12:08:09	12:14:33	384	
7,5	12:15:26	12:16:29	20	12:28:24	12:35:19	415	
			20	12:38:46	12:45:20	394	
			20	12:45:47	12:54:02	495	fel
5	12:55:45	12:57:16	20	13:03:26	13:12:48	562	
			20	13:15:51	13:22:50	419	
			20	13:23:21	13:30:20	419	
2,5	13:36:22	13:37:24	20	13:38:13	13:44:23	370	
			20	13:47:01	13:52:32	331	
Cycle 2			20	13:53:14	13:58:48	334	
10	13:59:58	14:01:01	20	14:02:33	14:11:42	549	
			20	14:16:30	14:26:04	574	
			20	14:26:25	14:36:00	575	
12,5	14:36:25	14:37:28	10	14:38:58	14:45:04	366	
			10	14:45:41	14:51:56	375	
			10	14:52:25	14:58:49	384	
15	14:59:52	15:00:30	10	15:03:27	15:11:28	481	
			10	15:12:17	15:20:28	491	
			10	15:20:54	15:29:15	501	
10	15:30:06	15:30:59	10,7	15:32:34	15:41:05	511	477
			10	15:43:14	15:51:07	473	
			10	15:51:45	15:59:36	471	
2,5	15:59:57	16:01:41	2	16:04:04	16:04:53	49	
			2	16:05:20	16:06:08	48	
Cycle 3			2	16:06:44	16:07:32	48	16:10: 47s
10	16:12:27	16:13:20	2	16:16:40	16:18:13	93	
			2	16:18:50	16:20:24	94	
			2	16:26:26	16:28:01	95	
15	16:28:27	16:29:01	2	16:32:49	16:34:45	116	
			2	16:36:57	16:38:58	121	
			2	16:41:13	16:43:13	120	
20	16:43:49	16:44:25	2	16:47:05	16:49:54	169	
			2	16:51:12	16:54:10	178	

			2	16:56:51	16:59:52	181	
10	17:01:07	17:02:08	2	17:03:31	17:06:01	150	
			2	17:07:21	17:09:48	147	
Cycle 4			2	17:13:10	17:15:39	149	
2,5	17:16:26	17:17:58	2	17:19:28	17:20:25	57	
			2	17:22:26	17:23:20	54	
			2	17:24:37	17:25:34	57	17:28: 57s
10	17:29:24	17:30:06	2	17:30:51	17:32:58	127	
			2	17:34:20	17:36:34	134	
			2	17:41:17	17:43:32	135	
20	17:43:59	17:44:31	2	17:45:41	17:49:10	209	
			2	17:49:46	17:53:17	211	
			2	17:53:50	17:57:25	215	
25	17:58:01	17:58:38	2	18:00:28	18:05:06	278	
			2	18:05:38	18:10:28	290	
			2	18:11:06	18:15:57	291	
10	18:16:27	18:17:58	2	18:19:19	18:22:44	205	
			2	18:23:08	18:26:31	203	
			2	18:27:20	18:31:03	223	
2,5	18:31:47	18:33:04	2	18:34:15	18:35:14	59	
			2	18:36:19	18:37:20	61	
			2	18:38:23	18:39:24	61	

Cycle: 1 Core: PS0037053

Pressure

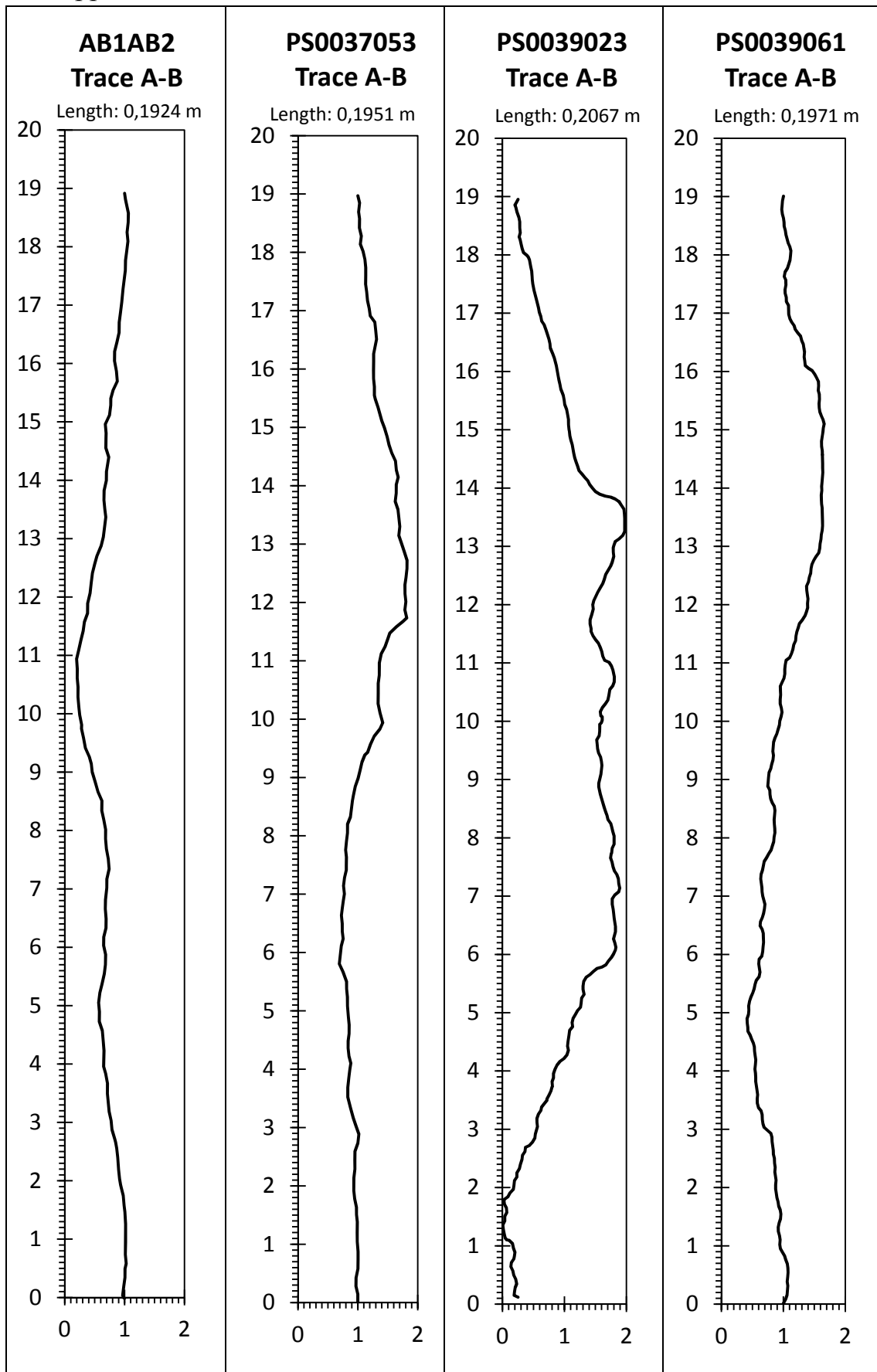
step (bar)	Adjustment started	Adjustment finished	Volume (ml)	Fill started	Fill finished	Fill time (s)	Notes
2,5	09:02:07	09:02:49	100	09:09:05	09:10:05	60	
		09:08:22	100	09:10:11	09:11:13	62	
			100	09:14:01	09:15:00	59	
5	09:15:50	09:16:09	100	09:18:26	09:20:02	96	
			100	09:20:12	09:21:50	98	
			100	09:24:37	09:26:20	103	
7,5	09:26:53	09:27:16	100	09:29:14	09:31:48	154	
			100	09:32:03	09:34:44	161	
			100	09:36:39	09:39:24	165	
10	09:39:53	09:40:16	100	09:43:48	09:47:37	229	
			100	09:48:01	09:52:01	240	
			100	09:52:31	09:56:39	248	
7,5	09:57:46	09:58:31	100	10:00:19	10:04:25	246	
			100	10:04:51	10:09:08	257	
			100	10:09:28	10:13:47	259	
5	10:14:28	10:15:14	100	10:16:23	10:20:32	249	
			100	10:20:58	10:25:08	250	
			110	10:25:35	10:30:15	280	
2,5	10:31:26	10:32:14	100	10:32:53	10:36:32	219	
			100	10:36:54	10:40:37	223	

			100	10:41:17	10:45:04	227	
Cycle 2			50	10:45:51	10:47:47	116	
10	10:48:18	10:48:45	50	10:50:24	10:53:24	180	
			50	10:53:52	10:56:54	182	
			50	10:57:13	11:00:18	185	
12,5	11:00:31	11:00:55	50	11:04:05	11:08:03	238	
			50	11:09:53	11:13:54	241	
			50	11:15:26	11:19:41	255	
15	11:20:05	11:20:33	50	11:22:08	11:27:21	313	
			50	11:27:36	11:32:56	320	
			50	11:33:10	11:38:33	323	
10	11:39:00	11:39:50	50	11:40:34	11:45:40	306	
			50	11:46:08	11:51:21	313	
			50	11:51:38	11:56:57	319	
2,5	11:57:16	11:58:38	50	11:59:16	12:02:43	207	
			50	12:03:04	12:06:32	208	
Cycle 3			50	12:06:57	12:10:30	213	
10	12:10:58	12:11:38	20	12:13:16	12:15:38	142	
			20	12:16:50	12:19:13	143	
			20	12:19:32	12:21:57	145	
15	12:22:27	12:23:02	20	12:24:21	12:27:18	177	
			20	12:28:47	12:31:44	177	
			20	12:31:59	12:34:55	176	
20	12:35:08	12:35:49	20	12:36:36	12:40:31	235	
			20	12:40:47	12:44:51	244	
			20	12:47:27	12:51:33	246	
10	12:51:49	12:52:53	20	12:53:37	12:57:09	212	
			20	12:57:25	13:00:58	213	
			20	13:02:51	13:06:27	216	
2,5	13:07:07	13:08:29	20	13:09:15	13:11:24	129	
			20	13:12:29	13:14:38	129	
Cycle 4			30	13:14:56	13:18:09	193	
10	13:19:27	13:20:01	20	13:21:13	13:24:46	213	
			20	13:26:32	13:30:04	212	
			20	13:33:18	13:36:45	207	
20	13:37:07	13:37:48	20	13:48:03	13:53:19	316	
			20	13:55:59	14:01:22	323	
			30	14:01:37	14:09:50	493	
25	14:11:06	14:11:54	10	14:12:19	14:15:43	204	
			10	14:16:10	14:19:30	200	
			10	14:30:41	14:34:26	225	
10	14:35:19	14:36:44	20	14:37:04	14:41:18	254	
			20	14:44:07	14:49:39	332	
			20	14:49:52	14:55:24	332	
2,5	14:55:43	14:57:01	20	14:57:45	15:00:51	186	
			20	15:01:09	15:03:43	154	
			20	15:05:17	15:08:20	183	

Cycle: 1 Core: PS0039023							
Pressure							
step (bar)	Adjustment started	Adjustment finished	Volume (ml)	Fill started	Fill finished	Fill time (s)	Notes
4	08:56:25	08:57:07	20	09:03:32	09:08:29	297	
			20	09:11:56	09:17:02	306	
			10	09:17:23	09:19:55	152	
5	09:20:21	09:20:42	10	09:21:29	09:24:25	176	
			10	09:24:53	09:27:51	178	
			10	09:28:30	09:31:33	183	
7,5	09:31:41	09:32:10	10	09:33:57	09:37:32	215	
			10	09:38:26	09:42:01	215	
			10	09:42:28	09:46:08	220	
10	09:46:34	09:46:55	20	09:47:13	09:54:39	446	
			30	09:54:55	10:06:53	718	
			10			0	
7,5	10:08:20	10:08:47	10	10:08:59	10:13:06	247	
			10	10:13:35	10:17:39	244	
			10	10:18:01	10:22:07	246	
5	10:22:46	10:23:07	10	10:23:54	10:27:51	237	
			10	10:28:14	10:32:07	233	
			10	10:32:29	10:36:23	234	
4	10:36:43	10:37:11	10	10:38:19	10:41:48	209	
			10	10:42:07	10:45:35	208	
Cycle 2			10	10:45:51	10:49:21	210	
10	10:49:53	10:50:03	10,87	10:51:07	10:55:34	267	245
			10	10:56:28	11:00:46	258	
			10	11:01:02	11:05:21	259	
12,5	11:05:55	11:06:17	10	11:06:53	11:11:25	272	
			10	11:11:45	11:16:17	272	
			10	11:16:34	11:21:11	277	
15	11:21:52	11:22:10	10	11:22:50	11:27:41	291	
			10	11:28:14	11:32:52	278	
			10	11:33:10	11:38:05	295	
10	11:38:51	11:39:20	11,34	11:39:58	11:45:28	330	291
			38	11:45:39	12:04:20	1121	295
			10	12:04:33	12:09:29	296	
4			10	12:12:17	12:16:26	249	
			10,72	12:16:44	12:21:06	262	244
Cycle 3			10	12:22:38	12:26:46	248	
10	12:27:08	12:27:28	10	12:28:29	12:33:13	284	
			10	12:33:36	12:38:29	293	
			10	12:39:08	12:44:04	296	
15	12:44:33	12:44:58	10	12:46:38	12:54:23	465	
			10	12:54:42	13:00:19	337	
			10	13:00:40	13:05:41	301	
20	13:06:01	13:06:27	11,04	13:06:40	13:12:44	364	330
			10	13:21:39	13:27:14	335	

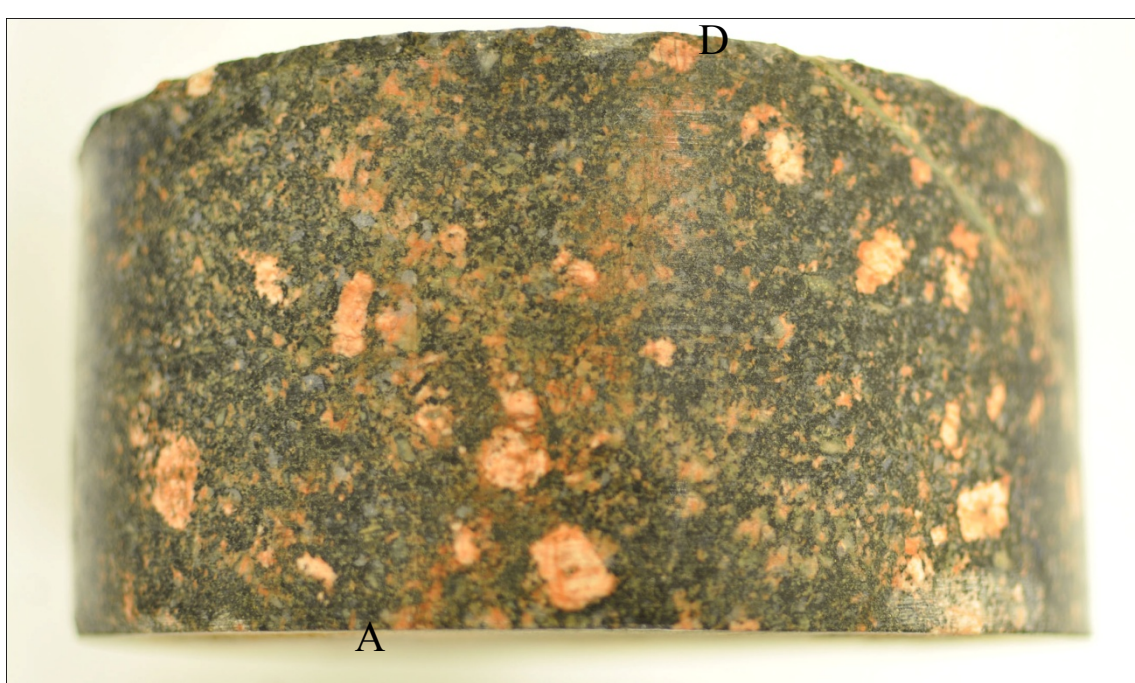
			11,07	13:27:30	13:33:43	373	337
10	13:34:42	13:35:22	10	13:35:43	13:41:12	329	
			10	13:41:32	13:47:18	346	
			10	13:47:35	13:53:06	331	
4	13:53:25	13:53:52	10	13:54:24	13:58:51	267	
			10	13:59:11	14:03:31	260	
Cycle 4			10	14:03:50	14:08:12	262	
10	14:08:36	14:08:55	10	14:09:23	14:14:34	311	
			10	14:14:51	14:20:08	317	
			10	14:20:25	14:25:43	318	
20	14:26:05	14:26:29	10	14:27:22	14:33:01	339	
			10	14:33:23	14:39:08	345	
			10	14:41:17	14:47:08	351	
25	14:47:36	14:48:03	11,02	14:49:08	14:55:58	410	370
			10	14:57:04	15:03:17	373	
			10,54	15:03:49	15:10:29	400	380
10	15:11:49	15:12:28	10	15:23:14	15:29:04	350	
			10	15:29:22	15:35:11	349	
			10,3	15:36:48	15:42:50	362	351
4	15:43:49	15:44:16	10	15:44:26	15:49:31	305	
			10	15:49:52	15:54:34	282	
			10,39	15:54:52	15:59:44	292	281

Appendix IV. Fracture traces

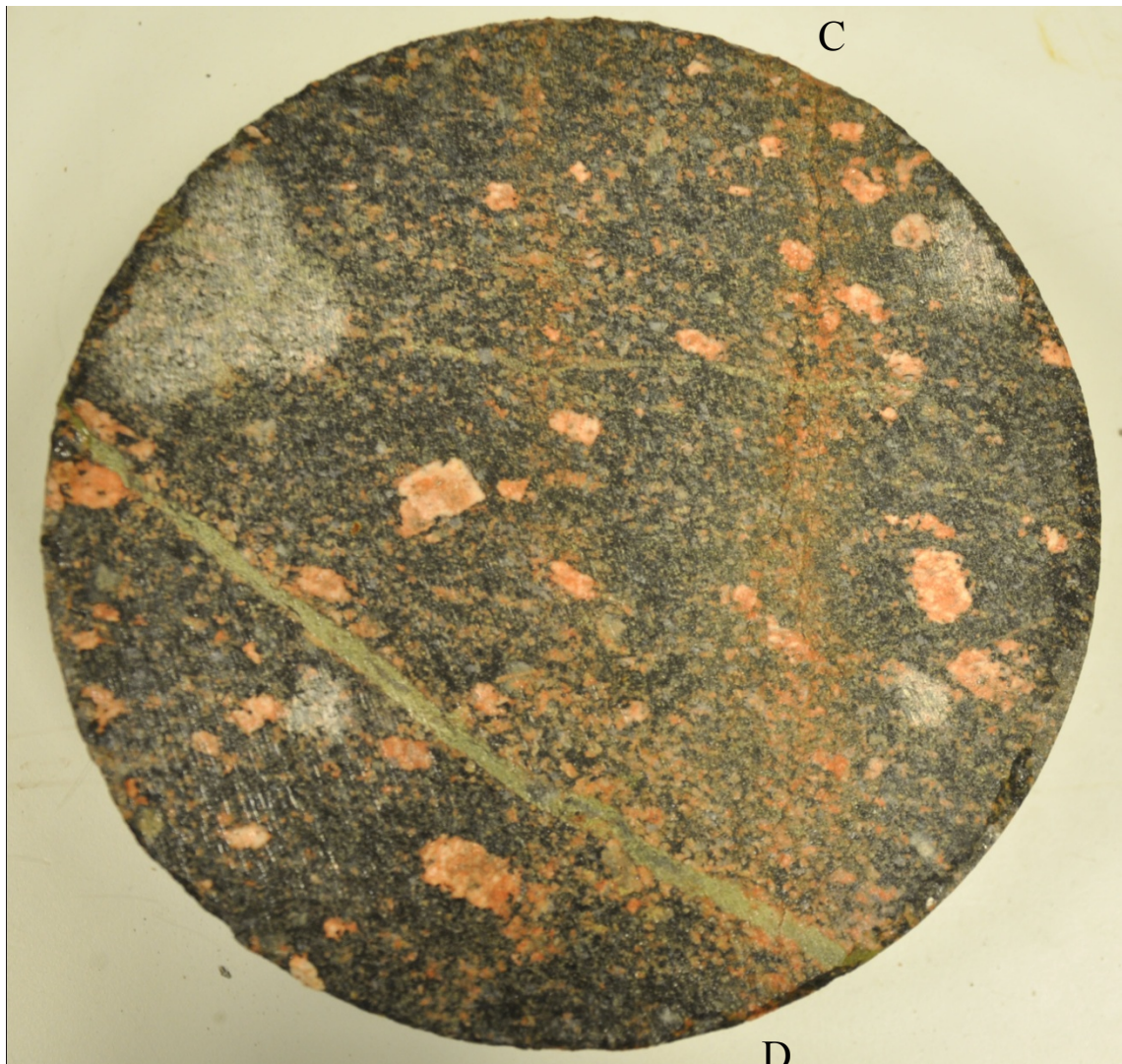


Appendix V. Photos of samples

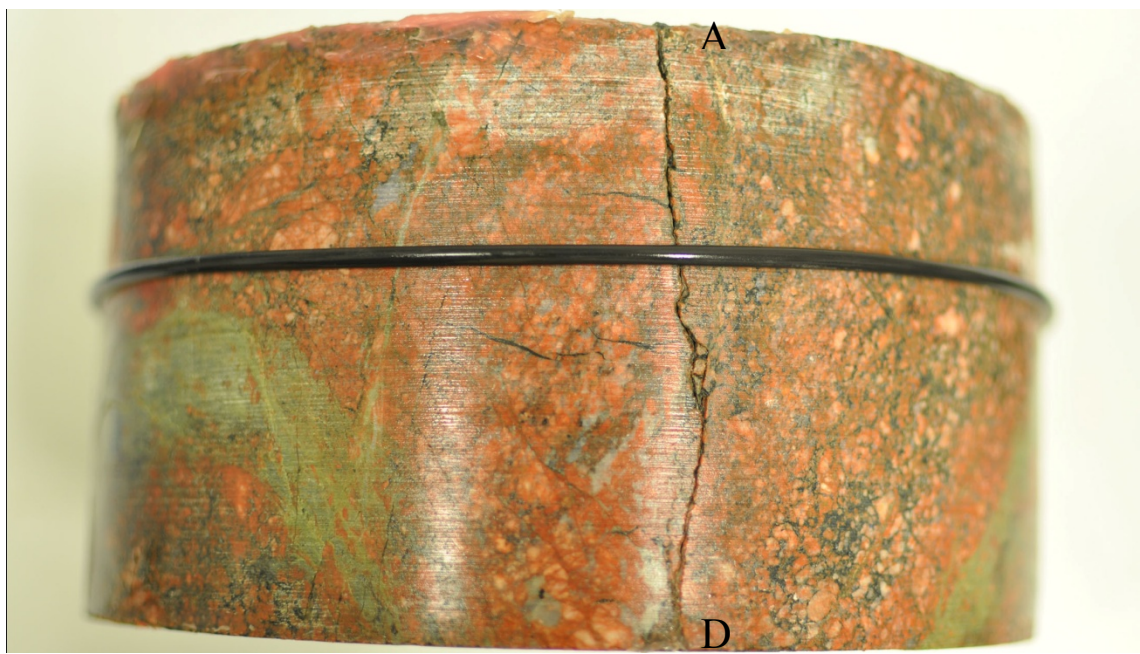
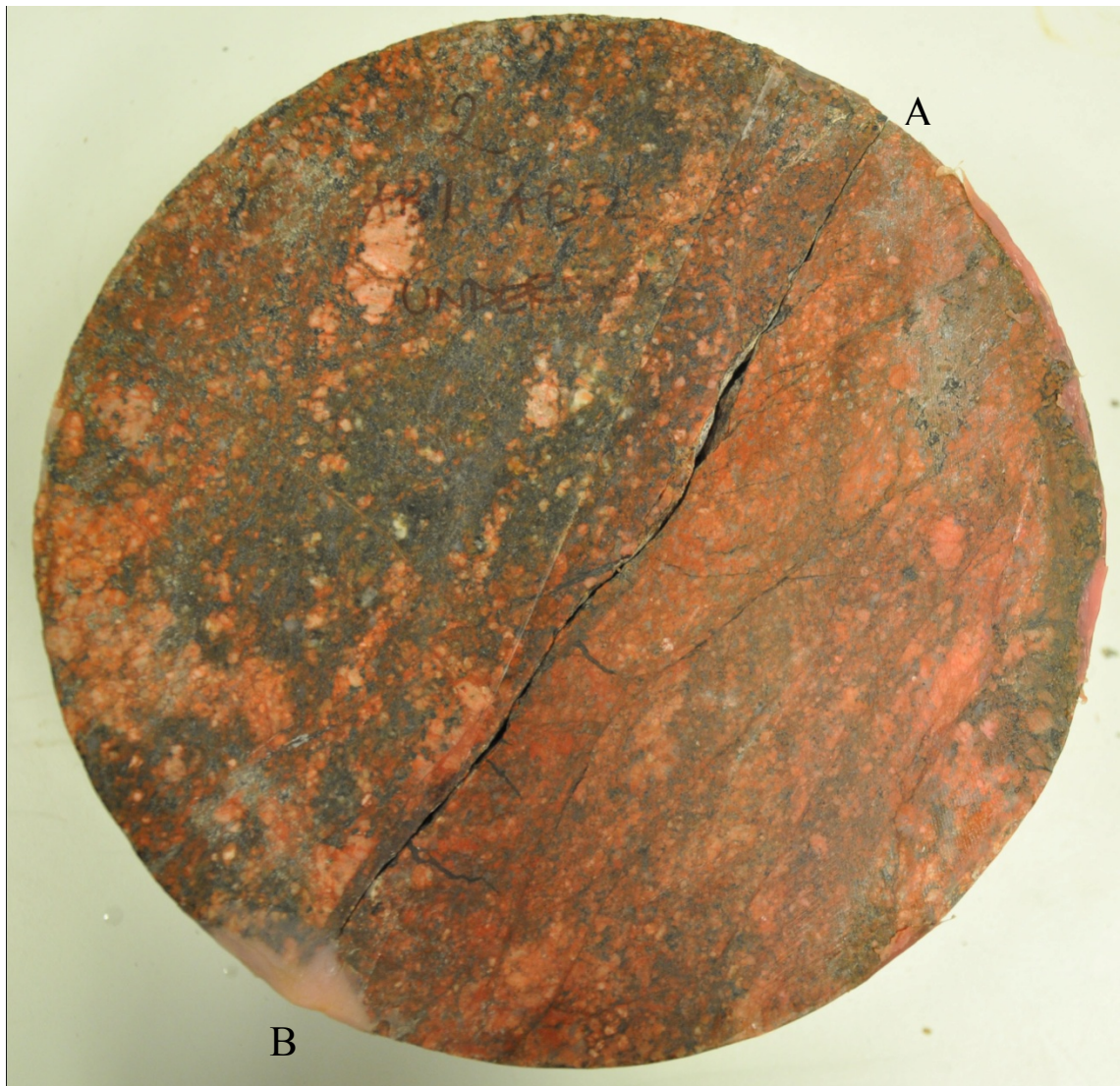
This appendix contains photos of the cores used in the experiments. The corners of the fairly rectangular fractures has been marked by A, B, C and D. The top side of most of the cores have shallow holes bored, where a steel plate was fastened when the samples were drilled from slabs. The steel plates have in most cases made rust staining on the surface. The fastening holes has been filled with silicone, which is smudged a bit around the holes, making the cores appear strange when wetted before photos were taken.



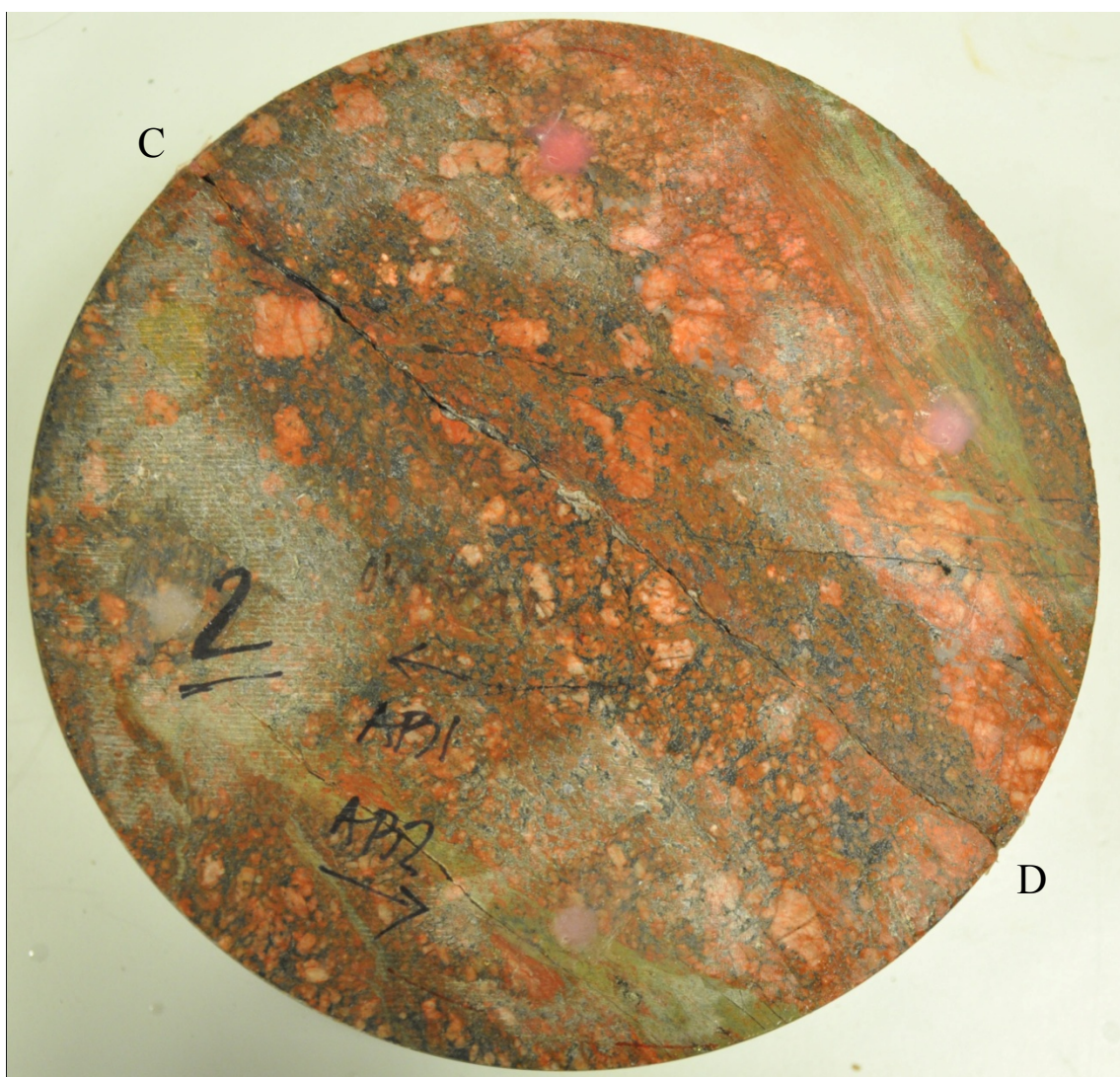
PS0039023. Fracture trace length A-B: 194.4 mm, height A-D: 98.1 mm



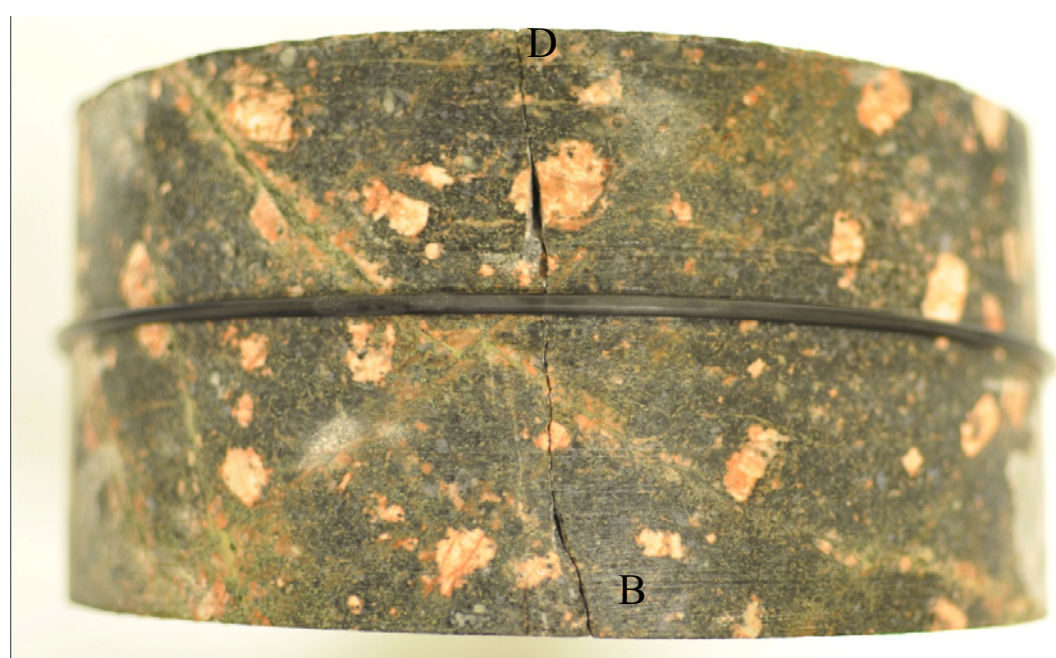
PS0039023. Fracture trace length C-D: 174.2 mm height C-B:102,5 mm



AB1AB2. Fracture length A-B: 192.3 mm, height A-D: 103.7 mm



AB1AB2. Fracture length C-D: 192.8 mm, height B-C:104.0 mm



PS0037053. Fracture length A-B:194.3 mm Height B-D: 94,2 mm



PS0037053. Fracture trace length C-D: 198,2 mm Trace height A-C: 97,5 mm

Appendix VI. **Analysis sheet PS0039061**

Coupling between changes in hydraulic and mechanical aperture*-Laboratory experiment*

20110120

Johan Thörn, PhD student, Division of GeoEngineering, Chalmers University of Technology

Input:

Parameter	Value	Unit	Note
Date:	20110120		
Time:	15-18		
Sample ID:	PS0039061		
Previous loadings:	5, 10, 7.5, 5, 2.5, 5, 7.5, 10, 20, 15, 10, 5, 10, 15, 20, 25, 20, 15, 10, 7.5, 5, 2.5 bar; 3 cycles		
T_w	20,4	[°C]	
T_{air}	21	[°C]	
V	-	[ml]	Volume of fracture
A	-	[cm ²]	Area of volume spread
dh	0,64	[m]	
ρ_w	998,141	[kg/m ³]	
g	9,81	[m/s ²]	
μ_w	0,001003	[Pas]	At 21°C

Flow:

Time [s]	V [ml]	p [MPa]	Q [m ³ /s]	T [m ² /s]	b [μm]	s [-]
226	200	0,5	8,87E-07	6,93E-07	94,8	4,62E-07
163	100	1	6,15E-07	4,80E-07	83,9	3,56E-07
159	100	0,75	6,28E-07	4,90E-07	84,5	3,61E-07
150	100	0,5	6,67E-07	5,21E-07	86,2	3,77E-07
129	100	0,25	7,75E-07	6,06E-07	90,6	4,20E-07
147	100	0,5	6,80E-07	5,31E-07	86,8	3,82E-07
164	100	0,75	6,11E-07	4,77E-07	83,7	3,54E-07
179	100	1	5,59E-07	4,36E-07	81,3	3,32E-07
267	100	1,5	3,75E-07	2,93E-07	71,1	2,50E-07
250	100	1	4,01E-07	3,13E-07	72,7	2,63E-07
205	100	0,5	4,89E-07	3,82E-07	77,7	3,02E-07
69	100	0,0	1,44E-06	1,13E-06	111,5	6,52E-07

Equations:

$$b_{hyd} = \sqrt[3]{\frac{12 \cdot \mu_w \cdot T}{\rho_w \cdot g}} \quad k_n = \frac{\rho_f \cdot g}{S}$$

$$S = 0,0109 \cdot T^{0,71}$$

Coupling between changes in hydraulic and mechanical aperture*-Laboratory experiment*

20110120

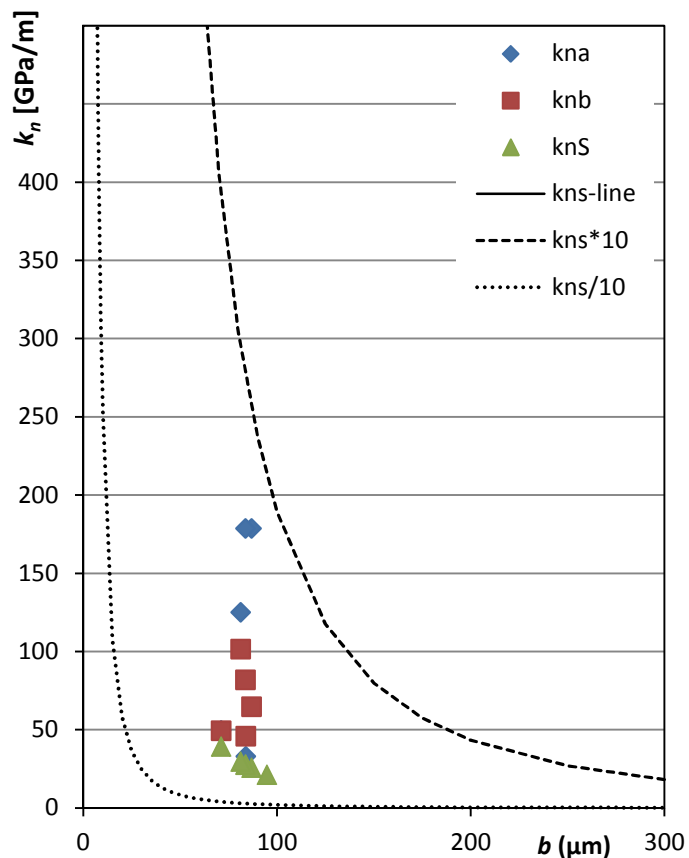
Johan Thörn, PhD student, Division of GeoEngineering, Chalmers University of Technology

Apertures:

p [MPa]	b_{hyd} [μm]	Δb [μm]	a [μm]	Δa [μm]	Δa/Δb [-]	Δa/Δb incr [-]
0,5	95	-	-	-	-	-
1	84	10,9	-	15,2	1,40	1,40
0,75	84	-0,6	-	0,5	-0,87	
0,5	86	-1,7	-	-0,3	0,17	
0,25	91	-4,4	-	-1,6	0,36	
0,5	87	3,9	-	1,4	0,36	0,36
0,75	84	3,1	-	1,4	0,46	0,46
1	81	2,5	-	2	0,81	0,81
1,5	71	10,1	-	10,1	1,00	1,00
1	73	-1,6	-	0,8	-0,50	
0,5	78	-5,0	-	-0,3	0,06	
0	111	-33,8	-	-25,2	0,75	

Stiffness:

k_n^a (Δσ'/Δa) [GPa/m]	k_n^b (Δσ'/Δb) [GPa/m]	k_n^s [GPa/m]
		21,2
32,9	45,9	27,5
-500,0	435,7	27,1
833,3	145,6	26,0
156,3	56,3	23,3
178,6	64,7	25,6
178,6	81,9	27,6
125,0	101,5	29,4
49,5	49,3	39,1
-625,0	310,7	37,3
1666,7	100,4	32,4
19,8	14,8	15,0

**Equations:**

$$b_{hyd} = \sqrt[3]{\frac{12 \cdot \mu_w \cdot T}{\rho_w \cdot g}} \quad k_n = \frac{\rho_f \cdot g}{S}$$

$$S = 0,0109 \cdot T^{0,71}$$

NOTE: values from decrease -steps not included

Coupling between changes in hydraulic and mechanical aperture*-Laboratory experiment*

20110120

Johan Thörn, PhD student, Division of GeoEngineering, Chalmers University of Technology

Flow/time calculations:

Time [mm:ss]	Time [s]	Volume [ml]	Volume [ml]	Flow [ml/s]	Cell pressure [bar]
00:03:47	227	200		0,881057	5
00:03:47	227	200		0,881057	5
00:03:43	223	200		0,896861	5
00:03:45	225	200		0,888889	5
00:05:17	317	200		0,630915	10
00:02:43	163	100		0,613497	10
00:02:44	164	100		0,609756	10
00:02:45	165	100		0,606061	10
00:02:38	158	100		0,632911	7,5
00:02:56	176	110		0,625	7,5
00:02:40	160	100		0,625	7,5
00:02:30	150	100		0,666667	5
00:02:30	150	100		0,666667	5
00:02:30	150	100		0,666667	5
00:02:09	129	100		0,775194	2,5
00:02:09	129	100		0,775194	2,5
00:02:09	129	100		0,775194	2,5
00:02:27	147	100		0,680272	5
00:02:27	147	100		0,680272	5
00:02:27	147	100		0,680272	5
00:02:44	164	100		0,609756	7,5
00:02:43	163	100		0,613497	7,5
00:02:44	164	100		0,609756	7,5
00:03:02	182	100		0,549451	10
00:02:57	177	100		0,564972	10
00:02:58	178	100		0,561798	10
00:04:24	264	100		0,378788	15
00:04:25	265	100		0,377358	15
00:04:32	272	100		0,367647	15
00:04:10	250	100		0,4	10
00:04:09	249	100		0,401606	10
00:04:10	250	100		0,4	10
00:03:24	204	100		0,490196	5
00:03:24	204	100		0,490196	5
00:03:26	206	100		0,485437	5
00:01:10	70	100		1,428571	0
00:01:09	69	100		1,449275	0
00:01:09	69	100		1,449275	0

Coupling between changes in hydraulic and mechanical aperture

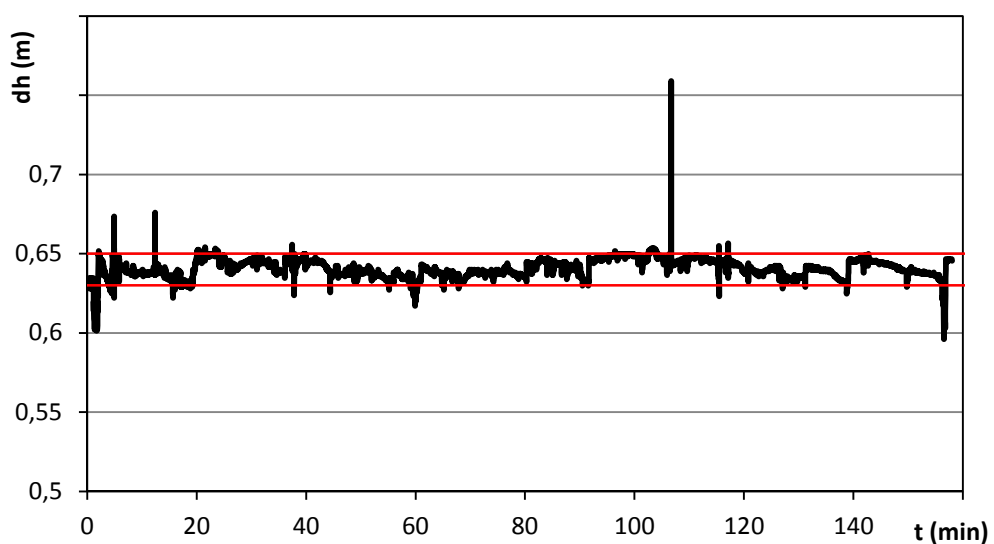
-Laboratory experiment

20110120

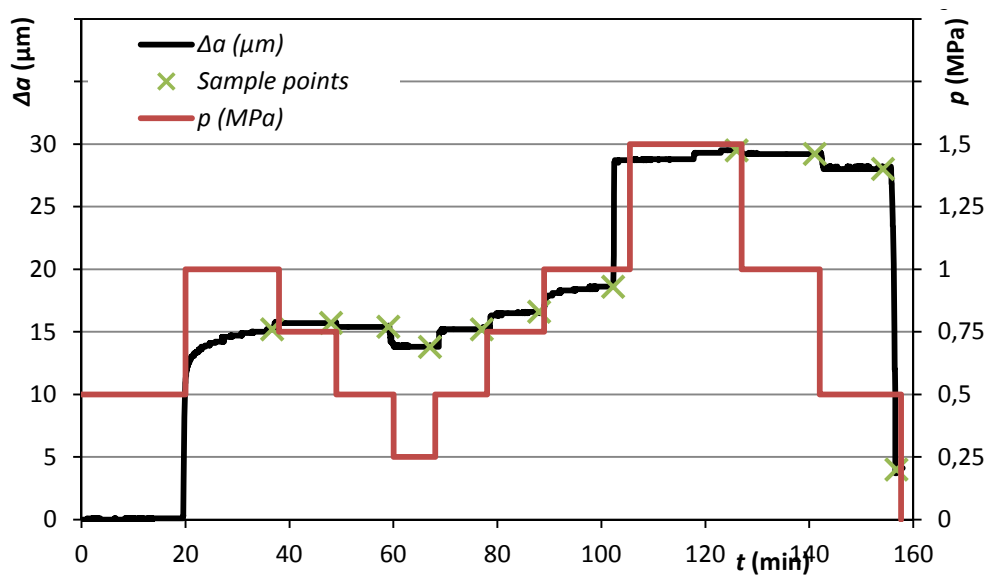
Johan Thörn, PhD student, Division of GeoEngineering, Chalmers University of Technology

dh reliability:

Set value	0,64 m	set value ± 1 cm	95,65%
no. Sec. < 0,63	270	2,85%	
no. Sec. > 0,65	142	1,50%	
total time	9480 s		
mean	0,6406 m		
stdev	0,00616 m		



Physical deformation:



Coupling between changes in hydraulic and mechanical aperture

-Laboratory experiment

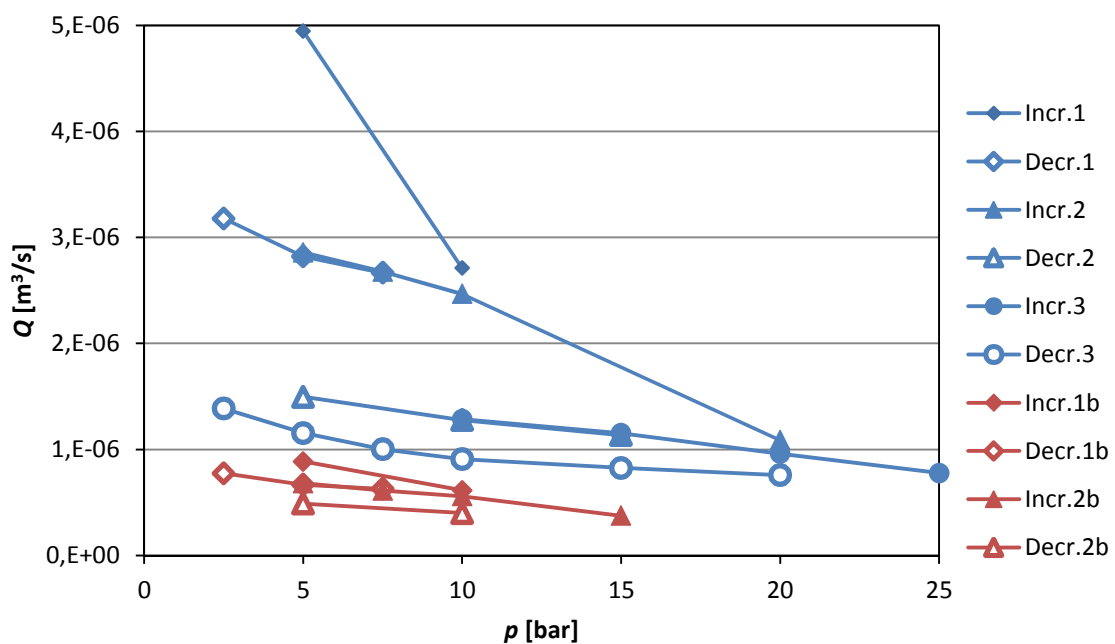
20110120

Johan Thörn, PhD student, Division of GeoEngineering, Chalmers University of Technology

Comparison SKB R-09-45:

Incr.1	Incr.2	Incr.3
5 4,946E-06	5 2,86E-06	10 1,287E-06
10 2,711E-06	7,5 2,68E-06	15 1,154E-06
	10 2,47E-06	20 9,610E-07
	20 1,09E-06	25 7,782E-07

Decr.1	Decr.2	Decr.3
7,5 2,667E-06	15 1,14E-06	20 7,576E-07
5 2,819E-06	10 1,28E-06	15 8,262E-07
2,5 3,178E-06	5 1,5E-06	10 9,093E-07
		7,5 1,003E-06
		5 1,156E-06
		2,5 1,385E-06



Incr.1b	Incr.2b
5 8,87E-07	5 6,80E-07
10 6,15E-07	7,5 6,11E-07
	10 5,59E-07
	15 3,75E-07

Decr.1b	Decr.2b
7,5 6,28E-07	10 4,01E-07
5 6,67E-07	5 4,89E-07
2,5 7,75E-07	

Coupling between changes in hydraulic and mechanical aperture

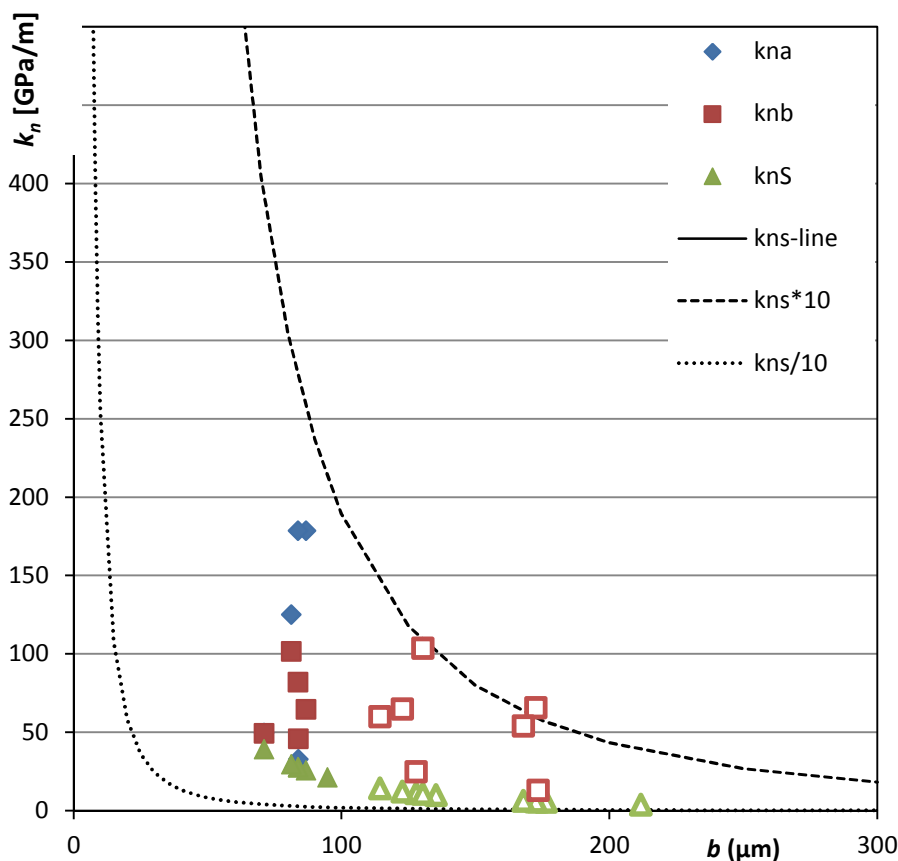
-Laboratory experiment

20110120

Johan Thörn, PhD student, Division of GeoEngineering, Chalmers University of Technology

Stiffness from SKB R-09-45 data:

p [bar]	Q [m^3/s]	T [m^2/s]	b [μm]	k_n^b [GPa/l]	k_n^s [GPa/m]
5	4,946E-06	7,727E-06	211,8		3,8
10	2,711E-06	4,237E-06	173,3	13	5,9
5	2,857E-06	4,464E-06	176,4		5,7
7,5	2,676E-06	4,181E-06	172,6	66	5,9
10	2,466E-06	3,853E-06	167,9	54	6,3
20	1,087E-06	1,698E-06	127,8	25	11,2
10	1,287E-06	2,011E-06	135,2		10,0
15	1,154E-06	1,803E-06	130,4	104	10,8
20	9,610E-07	1,502E-06	122,7	65	12,2
25	7,782E-07	1,216E-06	114,3	60	14,2



Note: Only values for increasing-pressure steps included

Appendix VII. Analysis sheet AB1AB2

Coupling between changes in hydraulic and mechanical aperture*-Laboratory experiment*

20110215

Johan Thörn, PhD student, Division of GeoEngineering, Chalmers University of Technology

Input:

	Parameter	Value	Unit	Note
	Date:	20110215		
	Time:	08-19		
	Sample ID:	AB1AB2		
	Previous loadings:	5, 10 bar		
Fracture	W	0,1925	[m]	Fracture width
	L	0,104	[m]	Fracture length
	V	-	[ml]	Volume of fracture
	A	-	[cm ²]	Area of volume spread
Conditions	T_w	20,5	[°C]	
	T_{air}	21	[°C]	Assumed
	dh	0,64	[m]	
	ρ_w	998,099	[kg/m ³]	at 20,5°C
	g	9,81	[m/s ²]	
	μ_w	0,000991	[Pas]	At 20,5°C
				JRC 11

Flow:

Time [s]	V [ml]	p [MPa]	Q	T	b	s
			[m ³ /s]	[m ² /s]	[μm]	[-]
417	100	0,25	2,40E-07	2,02E-07	62,6	1,93E-07
381	50	0,50	1,31E-07	1,11E-07	51,2	1,26E-07
672	50	0,75	7,44E-08	6,28E-08	42,4	8,40E-08
384	20	1,00	5,21E-08	4,40E-08	37,7	6,52E-08
394	20	0,75	5,08E-08	4,29E-08	37,3	6,40E-08
419	20	0,50	4,77E-08	4,03E-08	36,6	6,13E-08
334	20	0,25	5,99E-08	5,05E-08	39,4	7,20E-08
575	20	1,00	3,48E-08	2,94E-08	32,9	4,89E-08
384	10	1,25	2,60E-08	2,20E-08	29,9	3,98E-08
501	10	1,50	2,00E-08	1,68E-08	27,4	3,30E-08
471	10	1,00	2,12E-08	1,79E-08	27,9	3,45E-08
48	2	0,25	4,17E-08	3,52E-08	35,0	5,56E-08
95	2	1,0	2,11E-08	1,78E-08	27,8	3,43E-08
120	2	1,50	1,67E-08	1,41E-08	25,8	2,90E-08
181	2	2,00	1,10E-08	9,33E-09	22,5	2,17E-08
149	2	1,00	1,34E-08	1,13E-08	24,0	2,49E-08
57	2	0,25	3,51E-08	2,96E-08	33,0	4,92E-08
135	2	1,00	1,48E-08	1,25E-08	24,8	2,67E-08
215	2	2,00	9,30E-09	7,85E-09	21,2	1,92E-08
291	2	2,50	6,87E-09	5,80E-09	19,2	1,55E-08
223	2	1,00	8,97E-09	7,57E-09	21,0	1,87E-08
61	2	0,25	3,28E-08	2,77E-08	32,3	4,69E-08

Coupling between changes in hydraulic and mechanical aperture*-Laboratory experiment*

20110215

Johan Thörn, PhD student, Division of GeoEngineering, Chalmers University of Technology

Flow/time calculations:

Time [s]	Volume [ml]	p cell [bar]	Time [s]	Volume [ml]	p cell [bar]
377	100	2,5	93	2	10
404	100	2,5	94	2	10
417	100	2,5	95	2	10
353	50	5	116	2	15
373	50	5	121	2	15
381	50	5	120	2	15
616	50	7,5	169	2	20
645	50	7,5	178	2	20
672	50	7,5	181	2	20
387	20	10	150	2	10
402	20	10	147	2	10
384	20	10	149	2	10
415	20	7,5	57	2	2,5
394	20	7,5	54	2	2,5
495	20	7,5	57	2	2,5
562	20	5	127	2	10
419	20	5	134	2	10
419	20	5	135	2	10
370	20	2,5	209	2	20
331	20	2,5	211	2	20
334	20	2,5	215	2	20
549	20	10	278	2	25
574	20	10	290	2	25
575	20	10	291	2	25
366	10	12,5	205	2	10
375	10	12,5	203	2	10
384	10	12,5	223	2	10
481	10	15	59	2	2,5
491	10	15	61	2	2,5
501	10	15	61	2	2,5
477	10	10	49303	970	2,5
473	10	10	157	2	2,5
471	10	10		2	2,5
49	2	2,5	<i>The third time-value for each step has been used for further analysis.</i>		
48	2	2,5			
48	2	2,5			

Coupling between changes in hydraulic and mechanical aperture*-Laboratory experiment*

20110215

Johan Thörn, PhD student, Division of GeoEngineering, Chalmers University of Technology

Apertures:	1						
	<i>p</i> [MPa]	<i>b</i> [μm]	Δb [μm]	<i>a</i> [μm]	Δa [μm]	$\Delta a / \Delta b$	$\Delta a / \Delta b$ incr [-]
0,25	63	-	-	-	-	-	-
0,5	51	11,4	-	7,4	0,65	0,65	
0,75	42	8,8	-	4,7	0,53	0,53	
1	38	4,8	-	3,2	0,67	0,67	
0,75	37	0,3	-	-0,2	-0,62		
0,5	37	0,8	-	-0,1	-0,13		
0,25	39	-2,9	-	-1,8	0,63		
1	33	6,5	-	2,8	0,43	0,43	
1,25	30	3,0	-	1,6	0,53	0,53	
1,5	27	2,5	-	1,2	0,47	0,47	
1	28	-0,6	-	0,2	-0,35		
0,25	35	-7,0	-	-3,6	0,51		
1	28	7,1	-	3,1	0,44	0,44	
1,5	26	2,1	-	1,2	0,58	0,58	
2	22	3,3	-	1,6	0,49	0,49	
1	24	-1,5	-	-0,4	0,27		
0,25	33	-9,0	-	-4,8	0,53		
1	25	8,2	-	3,9	0,47	0,47	
2	21	3,6	-	2,1	0,59	0,59	
2,5	19	2,0	-	0,7	0,34	0,34	
1	21	-1,8	-	-0,4	0,22		
0,25	32	-11,3	-	-6,1	0,54		

Equations:

$$Q = \frac{V}{t}$$

$$S = 0,0109 \cdot T^{0,71}$$

$$T = \frac{Q \cdot L}{W \cdot dh}$$

$$k_n^s = \frac{\rho_w \cdot g}{S}$$

$$b = \sqrt[3]{\frac{12 \cdot \mu_w \cdot T}{\rho_w \cdot g}}$$

$$a = \sqrt{e \cdot JRC^{2,5}}$$

Coupling between changes in hydraulic and mechanical aperture

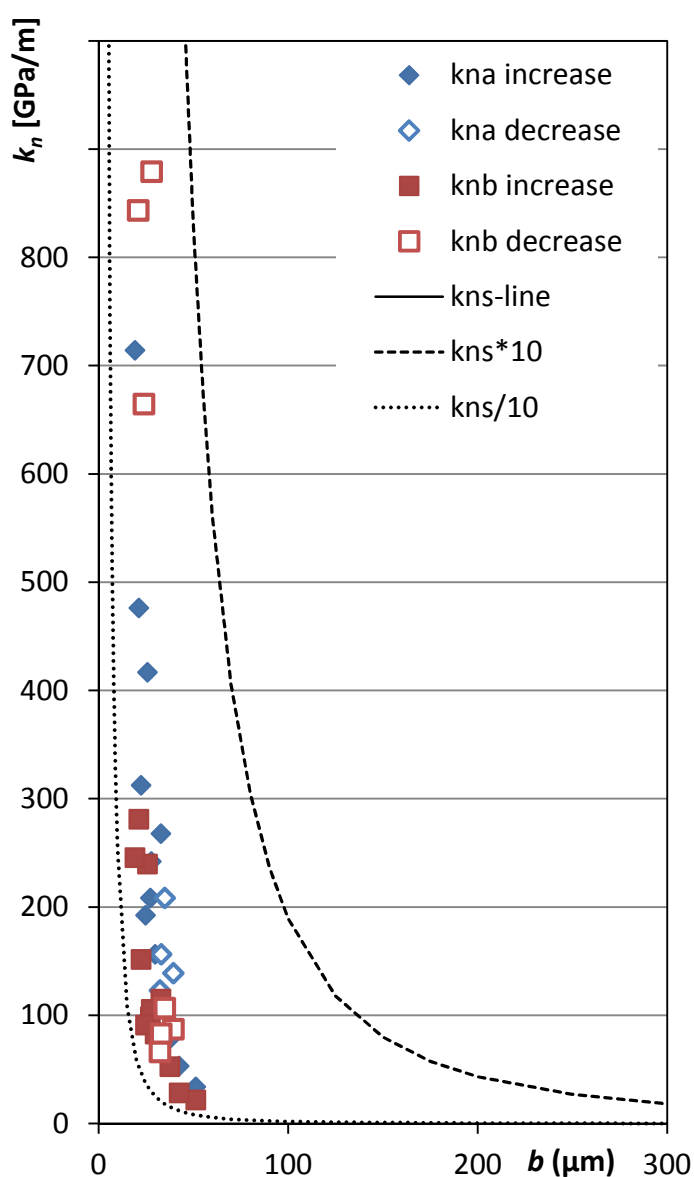
-Laboratory experiment

20110215

Johan Thörn, PhD student, Division of GeoEngineering, Chalmers University of Technology

Stiffness:

k_n^a ($\Delta\sigma'/\Delta a$) [GPa/m]	k_n^b ($\Delta\sigma'/\Delta b$) [GPa/m]	k_n^s [GPa/m]
		50,8
33,8	21,9	78,0
53,2	28,3	116,6
78,1	52,6	150,2
1250,0	-778,0	153,0
2500,0	-329,9	159,8
138,9	87,1	136,1
267,9	114,8	200,1
156,3	82,6	245,8
208,3	98,6	296,9
-2500,0	879,0	284,1
208,3	106,6	176,0
241,9	105,4	285,8
416,7	239,7	337,4
312,5	151,6	451,7
2500,0	664,6	393,4
156,3	82,9	198,9
192,3	91,0	366,8
476,2	281,0	510,5
714,3	245,7	632,8
3750,0	843,4	523,9
123,0	66,2	208,7

increase-steps in **bold**

Coupling between changes in hydraulic and mechanical aperture

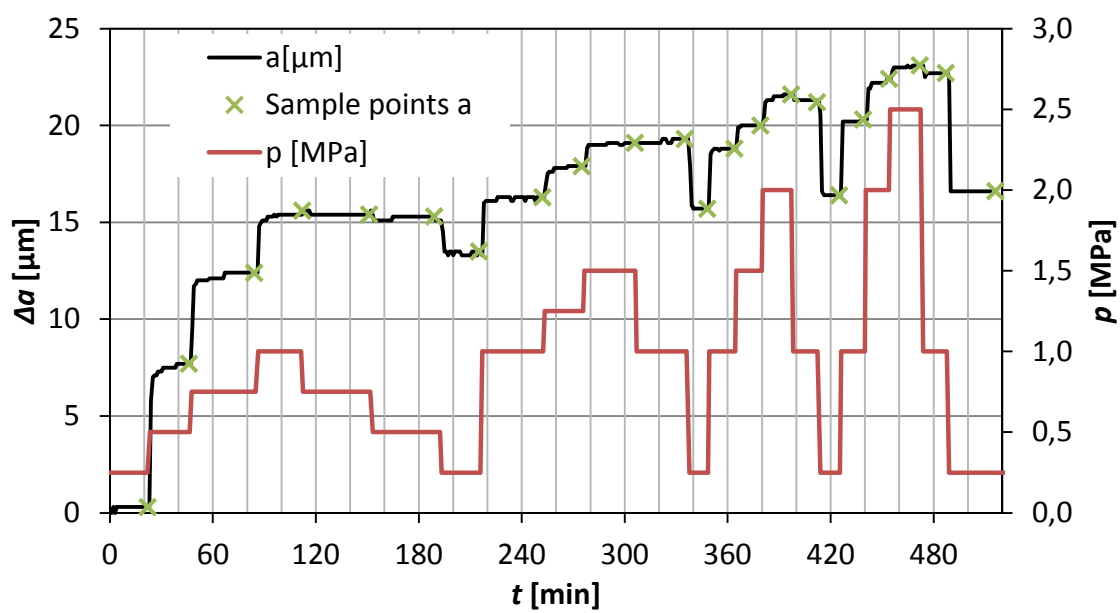
-Laboratory experiment

20110215

Johan Thörn, PhD student, Division of GeoEngineering, Chalmers University of Technology

Physical deformation:

<i>t</i> [min]	<i>a</i> [μm]	<i>p</i> [MPa]	Δa [μm]
22	0,3	0,25	
46	7,7	0,5	7,4
84	12,4	0,75	4,7
111	15,6	1	3,2
151	15,4	0,75	-0,2
189	15,3	0,5	-0,1
215	13,5	0,25	-1,8
252	16,3	1	2,8
275	17,9	1,25	1,6
306	19,1	1,5	1,2
335	19,3	1	0,2
348	15,7	0,25	-3,6
364	18,8	1	3,1
379	20	1,5	1,2
397	21,6	2	1,6
412	21,2	1	-0,4
425	16,4	0,25	-4,8
439	20,3	1	3,9
454	22,4	2	2,1
472	23,1	2,5	0,7
487	22,7	1	-0,4
516	16,6	0,25	-6,1



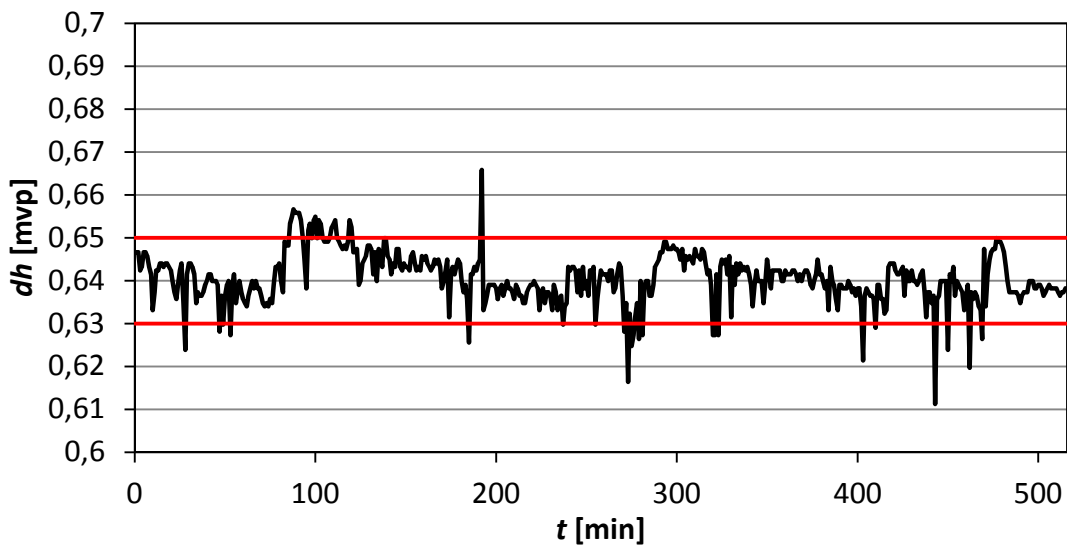
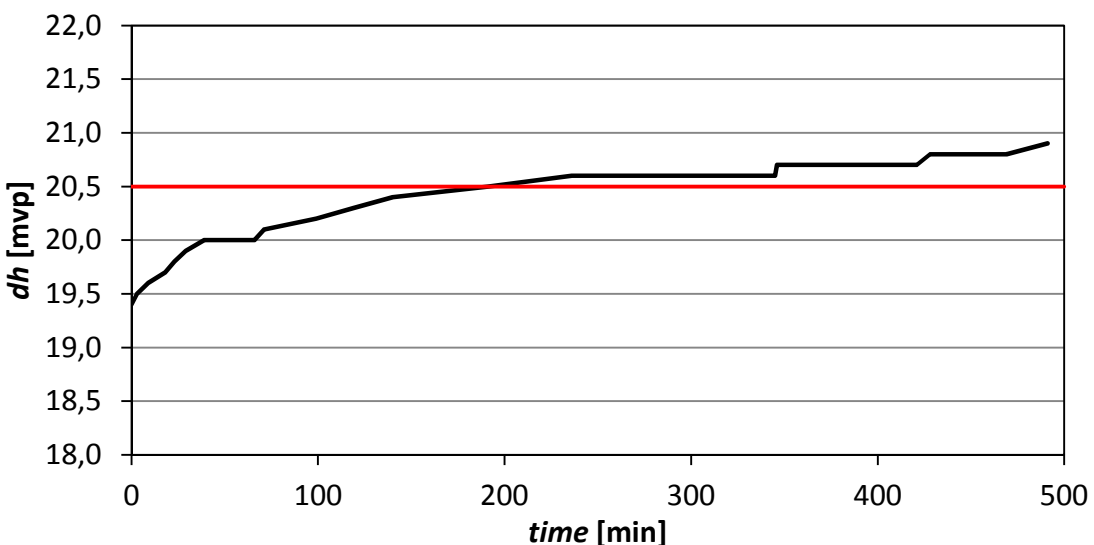
Coupling between changes in hydraulic and mechanical aperture*-Laboratory experiment*

20110215

Johan Thörn, PhD student, Division of GeoEngineering, Chalmers University of Technology

***dh* reliability:**

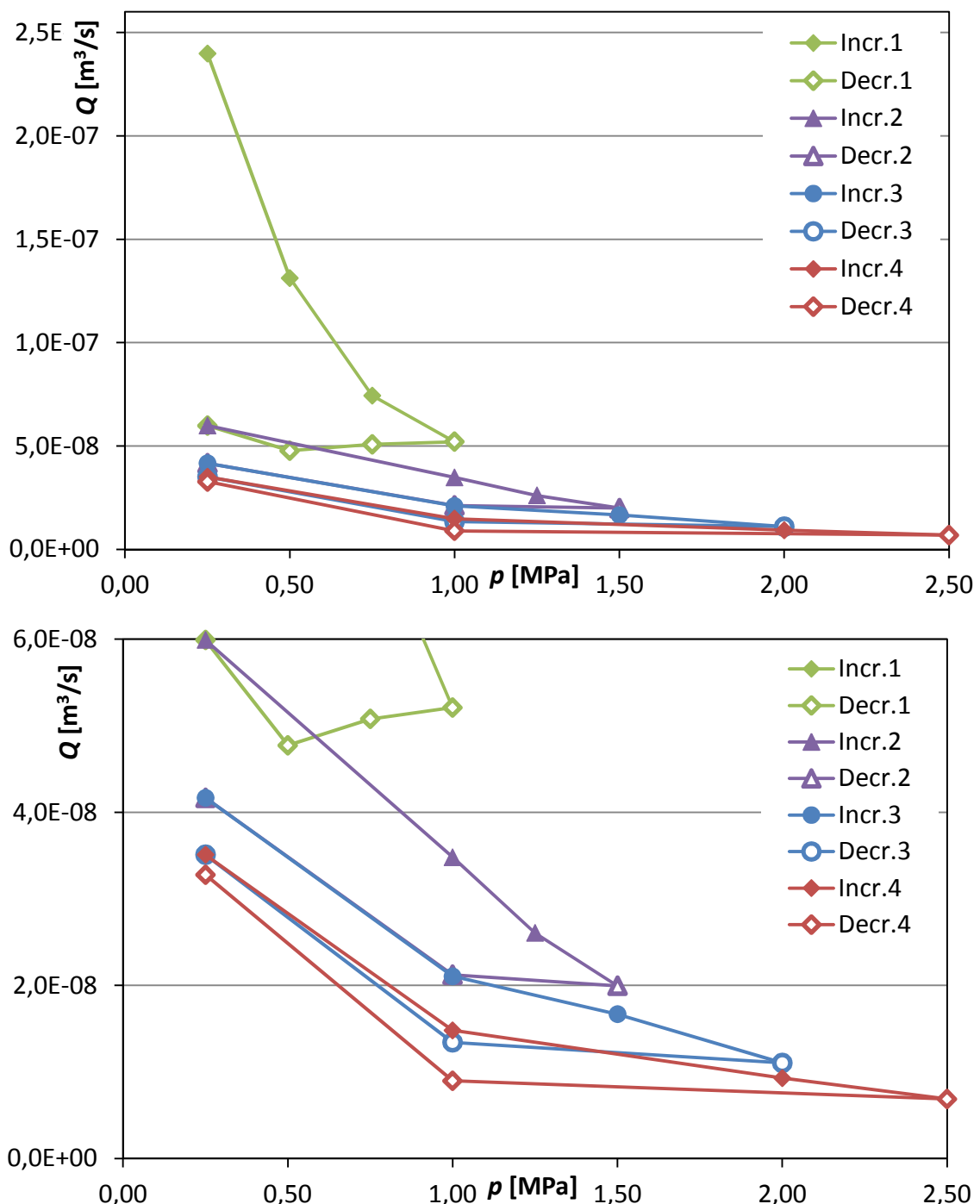
Set value	0,64 m	set value ± 1 cm	92,14%
no. Sec. < 0,63	1073 s	3,47%	
no. Sec. > 0,65	1361 s	4,40%	
total time	30960 s		
mean	0,640665 m		
stdev	0,005639 m		

***t_w* reliability:**

Coupling between changes in hydraulic and mechanical aperture*-Laboratory experiment*

20110215

Johan Thörn, PhD student, Division of GeoEngineering, Chalmers University of Technology

Flow-pressure graphs

Appendix VIII. Analysis sheet PS0037053

Coupling between changes in hydraulic and mechanical aperture*-Laboratory experiment*

20110224

Johan Thörn, PhD student, Division of GeoEngineering, Chalmers University of Technology

Input:

	Parameter	Value	Unit	Note
	Date:	20110224		
	Time:	07-16		
	Sample ID:	PS0037053		
	Previous loadings:	5, 10 bar		
Fracture	W	0,196 [m]		Fracture width
	L	0,096 [m]		Fracture length
	V	- [ml]		Volume of fracture
	A	- [cm ²]		Area of volume spread
Conditions	T_w	20 [°C]		
	T_{air}	21 [°C]		Assumed
	dh	0,66 [m]		
	ρ_w	998,203 [kg/m ³]		at 20.0°C
	g	9,81 [m/s ²]		
	μ_w	0,001003 [Pas]		At 20.0°C

Flow:

Time [s]	V [ml]	p [MPa]	Q	T	b	s
			[m ³ /s]	[m ² /s]	[μm]	[-]
60	100	0,25	1,67E-06	1,24E-06	115,0	6,97E-07
103	100	0,50	9,71E-07	7,21E-07	96,0	4,75E-07
165	100	0,75	6,06E-07	4,50E-07	82,1	3,40E-07
248	100	1,00	4,03E-07	2,99E-07	71,6	2,54E-07
259	100	0,75	3,86E-07	2,87E-07	70,6	2,47E-07
250	100	0,50	4,00E-07	2,97E-07	71,5	2,53E-07
227	100	0,25	4,41E-07	3,27E-07	73,8	2,71E-07
180	50	1,00	2,78E-07	2,06E-07	63,3	1,95E-07
240	50	1,25	2,08E-07	1,55E-07	57,5	1,59E-07
323	50	1,50	1,55E-07	1,15E-07	52,1	1,29E-07
319	50	1,00	1,57E-07	1,16E-07	52,3	1,30E-07
213	50	0,25	2,35E-07	1,74E-07	59,8	1,73E-07
145	20	1,0	1,38E-07	1,02E-07	50,1	1,19E-07
176	20	1,50	1,14E-07	8,43E-08	47,0	1,03E-07
246	20	2,00	8,13E-08	6,03E-08	42,0	8,16E-08
212	20	1,00	9,43E-08	7,00E-08	44,1	9,07E-08
129	20	0,25	1,55E-07	1,15E-07	52,1	1,29E-07
213	20	1,00	9,39E-08	6,97E-08	44,1	9,04E-08
493	30	2,00	6,09E-08	4,52E-08	38,1	6,64E-08
225	10	2,50	4,44E-08	3,30E-08	34,4	5,31E-08
332	20	1,00	6,02E-08	4,47E-08	38,0	6,59E-08
183	20	0,25	1,09E-07	8,11E-08	46,4	1,01E-07

Coupling between changes in hydraulic and mechanical aperture*-Laboratory experiment*

20110224

Johan Thörn, PhD student, Division of GeoEngineering, Chalmers University of Technology

Flow/time calculations:

Time [s]	Volume [ml]	p cell [bar]	Time [s]	Volume [ml]	p cell [bar]
60	100	2,5	142	20	10
62	100	2,5	143	20	10
59	100	2,5	145	20	10
96	100	5	177	20	15
98	100	5	177	20	15
103	100	5	176	20	15
154	100	7,5	235	20	20
161	100	7,5	244	20	20
165	100	7,5	246	20	20
229	100	10	212	20	10
240	100	10	213	20	10
248	100	10	216	20	10
246	100	7,5	129	20	2,5
257	100	7,5	129	20	2,5
259	100	7,5	193	30	2,5
249	100	5	213	20	10
250	100	5	212	20	10
280	110	5	207	20	10
219	100	2,5	316	20	20
223	100	2,5	323	20	20
227	100	2,5	493	30	20
180	50	10	204	10	25
182	50	10	200	10	25
185	50	10	225	10	25
238	50	12,5	254	20	10
241	50	12,5	332	20	10
255	50	12,5	332	20	10
313	50	15	186	20	2,5
320	50	15	154	20	2,5
323	50	15	183	20	2,5
306	50	10			
313	50	10			
319	50	10			
207	50	2,5	<i>The third time-value for each step has been used for further analysis.</i>		
208	50	2,5			
	50	2,5			

Coupling between changes in hydraulic and mechanical aperture*-Laboratory experiment*

20110224

Johan Thörn, PhD student, Division of GeoEngineering, Chalmers University of Technology

Apertures:

p [MPa]	b [μm]	Δb [μm]	a [μm]	Δa [μm]	Δa/Δb [-]	Δa/Δb incr [-]
0,25	115	-	-	-	-	-
0,5	96	19,0	-	25	1,31	1,31
0,75	82	14,0	-	19	1,39	1,39
1	72	10,4	-	16	1,57	1,57
0,75	71	1,0	-	-1	-0,78	
0,5	71	-0,8	-	-2	2,75	
0,25	74	-2,3	-	-6	2,57	
1	63	10,5	-	14	1,29	1,29
1,25	57	5,8	-	12	2,13	2,13
1,5	52	5,4	-	11	1,97	1,97
1	52	-0,2	-	-2	7,84	
0,25	60	-7,5	-	-14	1,80	
1	50	9,7	-	12	1,22	1,22
1,5	47	3,1	-	8	2,55	2,55
2	42	5,0	-	15	3,00	3,00
1	44	-2,1	-	-4	1,87	
0,25	52	-8,0	-	-16	1,97	
1	44	8,0	-	12	1,46	1,46
2	38	5,9	-	14	2,31	2,31
2,5	34	3,8	-	11	2,79	2,79
1	38	-3,7	-	-6	1,72	
0,25	46	-8,3	-	-17	2,05	

Equations:

$$Q = \frac{V}{t}$$

$$S = 0,0109 \cdot T^{0,71}$$

$$T = \frac{Q \cdot L}{W \cdot dh}$$

$$k_n^S = \frac{\rho_w \cdot g}{S}$$

$$b = \sqrt[3]{\frac{12 \cdot \mu_w \cdot T}{\rho_w \cdot g}}$$

Coupling between changes in hydraulic and mechanical aperture

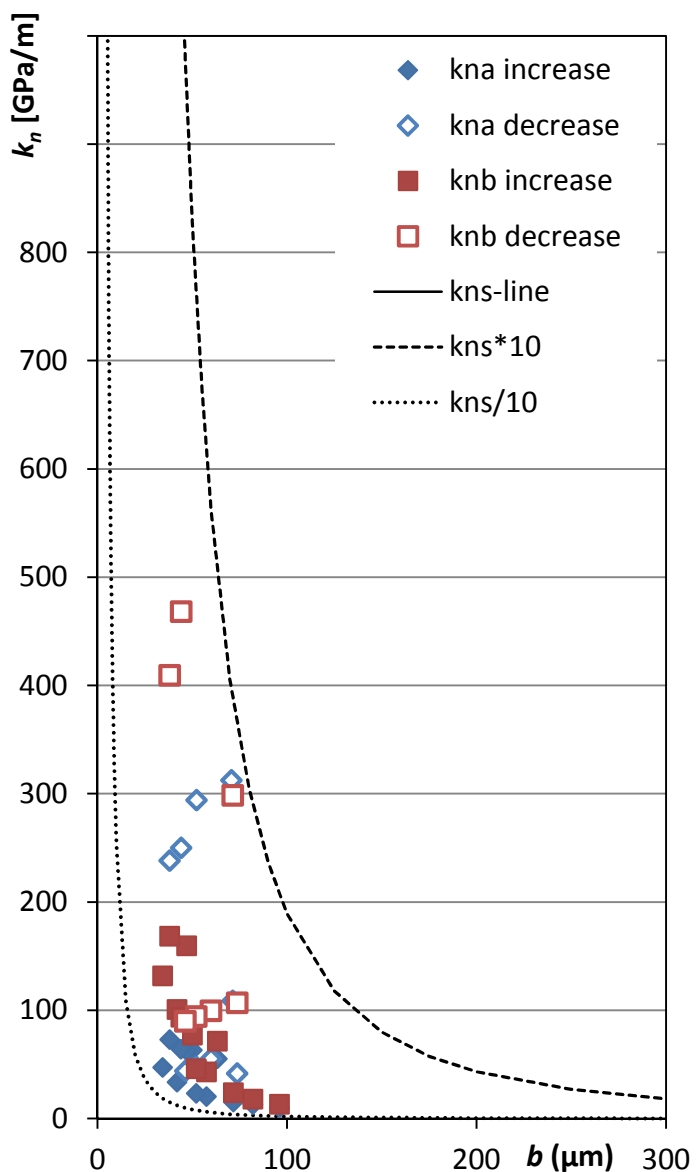
-Laboratory experiment

20110224

Johan Thörn, PhD student, Division of GeoEngineering, Chalmers University of Technology

Stiffness:

k_n^a ($\Delta\sigma'/\Delta a$) [GPa/m]	k_n^b ($\Delta\sigma'/\Delta b$) [GPa/m]	k_n^s [GPa/m]
10,1	13,2	20,6
12,9	17,9	28,8
15,2	24,0	38,5
312,5	-242,9	39,7
108,7	298,5	38,7
41,7	107,0	36,2
55,1	71,3	50,2
20,3	43,2	61,5
23,4	46,1	76,0
294,1	2306,8	75,3
55,1	99,5	56,5
63,0	77,2	82,5
62,5	159,5	94,6
33,6	100,8	120,0
250,0	468,3	108,0
47,8	94,3	75,9
64,1	93,5	108,4
73,0	168,5	147,4
47,2	131,8	184,3
238,1	409,3	148,5
43,9	89,8	97,3

increase-steps in **bold**

Coupling between changes in hydraulic and mechanical aperture

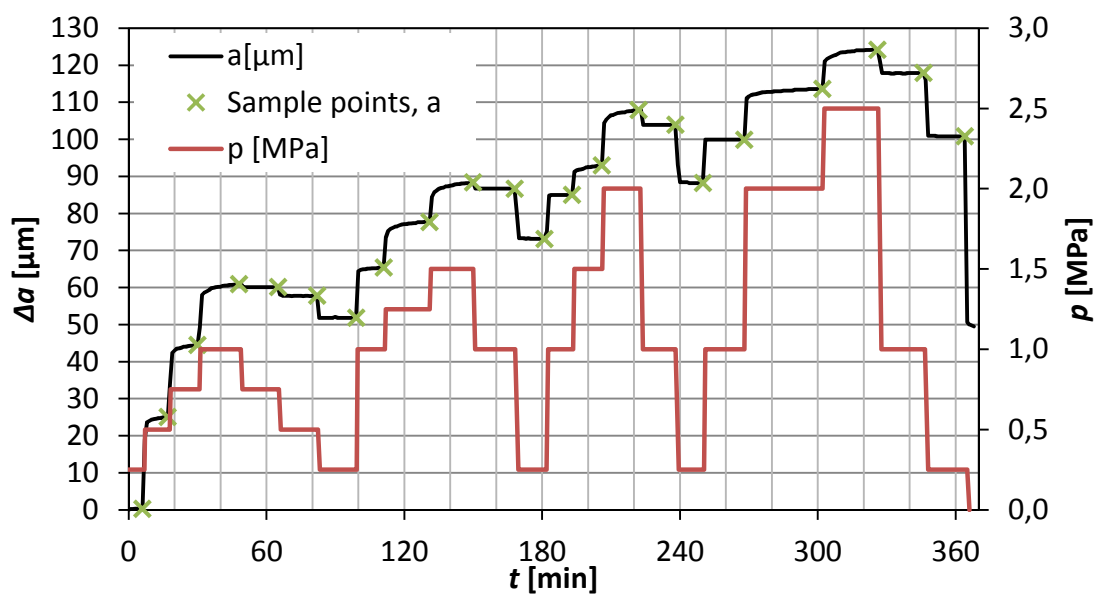
-Laboratory experiment

20110224

Johan Thörn, PhD student, Division of GeoEngineering, Chalmers University of Technology

Physical deformation:

<i>t</i> [min]	<i>a</i> [μm]	<i>p</i> [MPa]	Δa [μm]
6	0	0,25	
17	25	0,5	25
30	45	0,75	19,4
48	61	1	16,4
65	60	0,75	-0,8
82	58	0,5	-2,3
99	52	0,25	-6
111	65	1	13,6
131	78	1,25	12,3
150	88	1,5	10,7
168	87	1	-1,7
181	73	0,25	-13,6
193	85	1	11,9
206	93	1,5	8
222	108	2	14,9
238	104	1	-4
250	88	0,25	-15,7
268	100	1	11,7
302	114	2	13,7
326	124	2,5	10,6
346	118	1	-6,3
364	101	0,25	-17,1



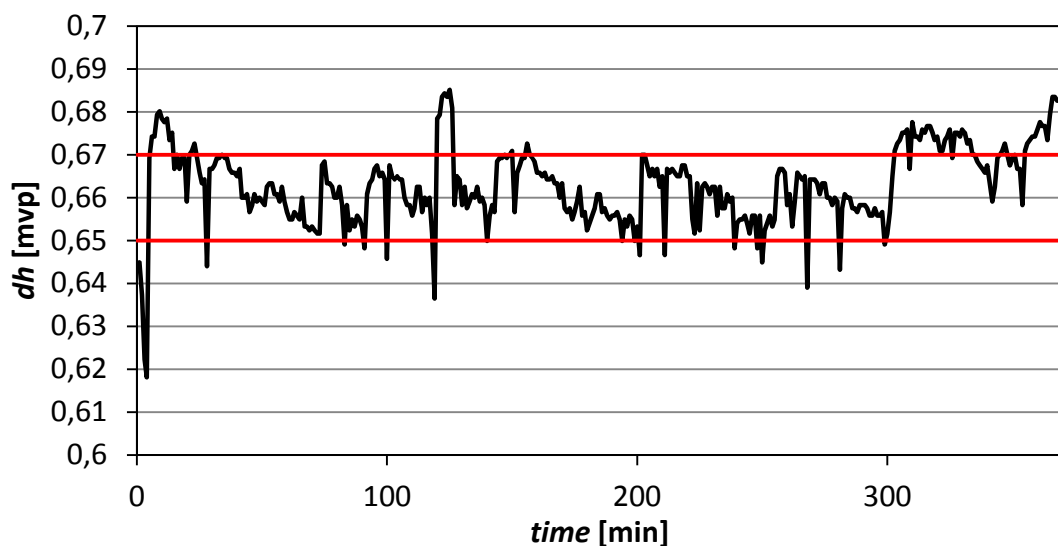
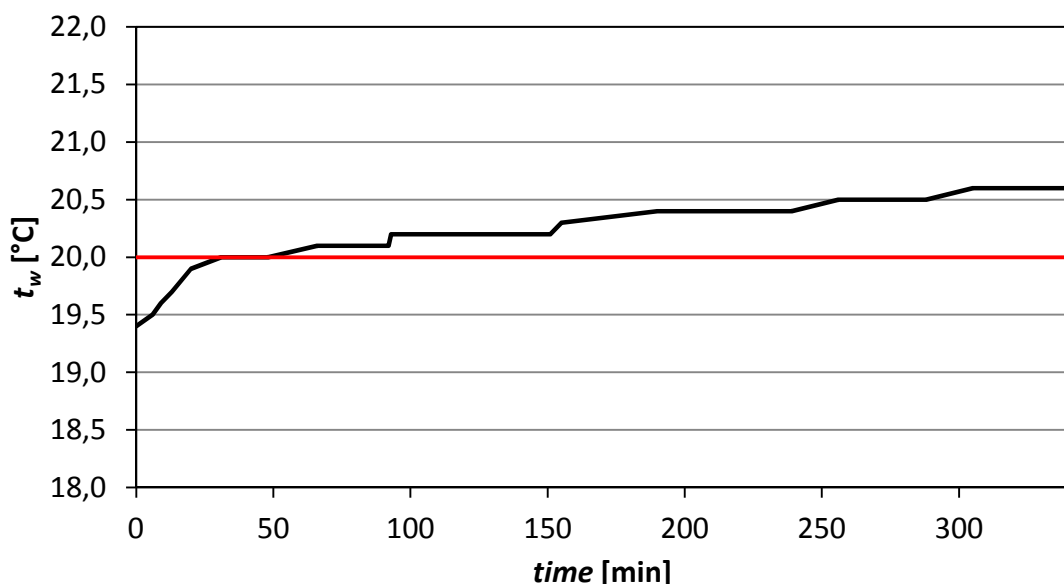
Coupling between changes in hydraulic and mechanical aperture*-Laboratory experiment*

20110224

Johan Thörn, PhD student, Division of GeoEngineering, Chalmers University of Technology

***dh* reliability:**

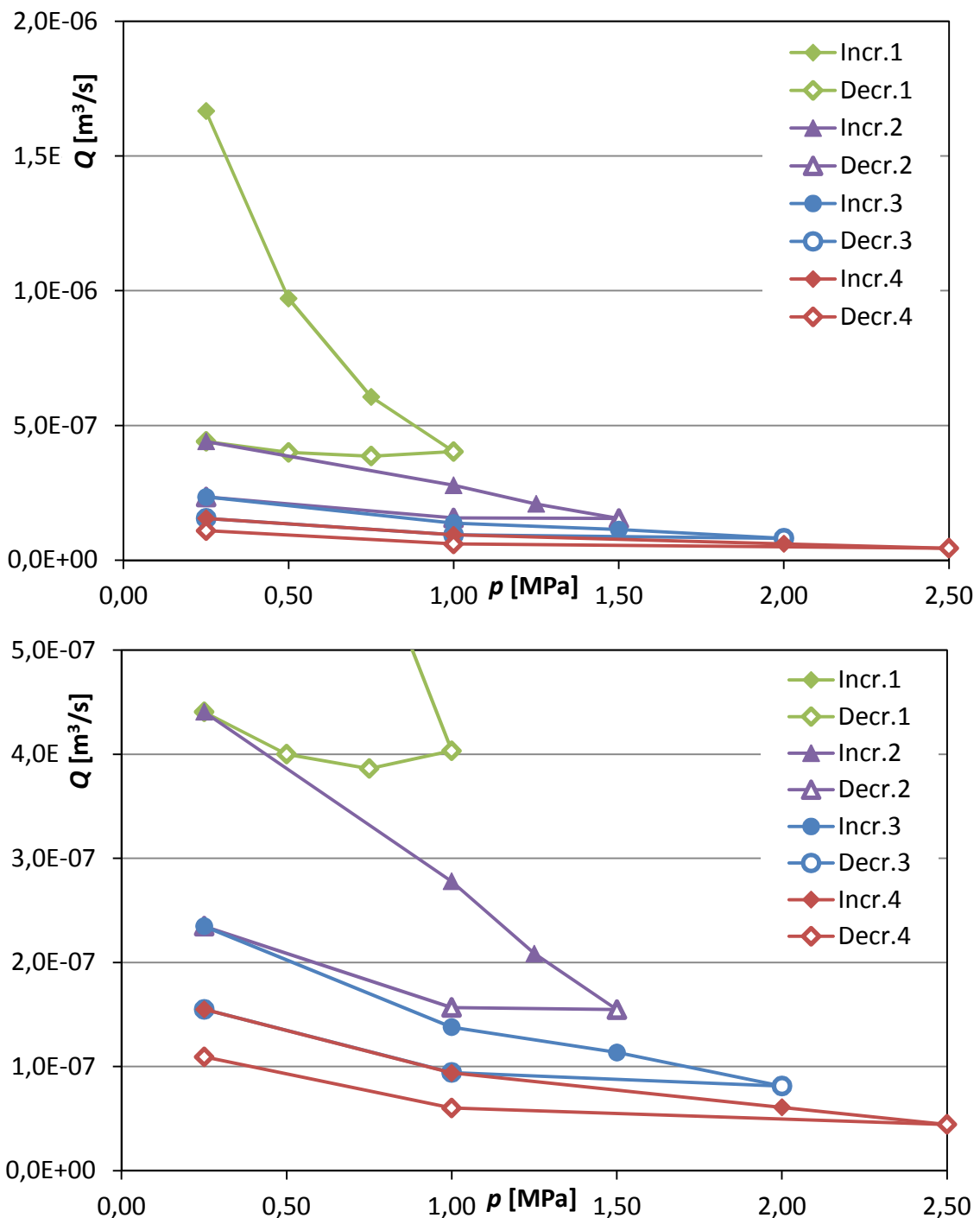
Set value	0,66 m	set value ± 1 cm	76,93%
no. Sec. < 0,65	1154 s	5,22%	
no. Sec. > 0,67	3950 s	17,85%	
total time	22123 s		
mean	0,6627785 m		
stdev	0,0091295 m		

***t_w* reliability:**

Coupling between changes in hydraulic and mechanical aperture*-Laboratory experiment*

20110224

Johan Thörn, PhD student, Division of GeoEngineering, Chalmers University of Technology

Flow-pressure graphs

Appendix IX. **Analysis sheet PS0039023**

Coupling between changes in hydraulic and mechanical aperture*-Laboratory experiment*

20110301

Johan Thörn, PhD student, Division of GeoEngineering, Chalmers University of Technology

Input:

	Parameter	Value	Unit	Note
	Date:	20110301		
	Time:	07-16		
	Sample ID:	PS0039023		
	Previous loadings:	5, 10 bar		
Fracture	W	0,184	[m]	Fracture width
	L	0,1	[m]	Fracture length
	V	-	[ml]	Volume of fracture
	A	-	[cm ²]	Area of volume spread
Conditions	T_w	20	[°C]	
	T_{air}	21	[°C]	Assumed
	dh	35,1	[m]	
	ρ_w	998,203	[kg/m ³]	at 20.0°C
	g	9,81	[m/s ²]	
	μ_w	0,001003	[Pas]	At 20.0°C

Flow:

Time [s]	V [ml]	p [MPa]	Q	T	b	s
			[m ³ /s]	[m ² /s]	[μm]	[-]
152	10	0,40	6,58E-08	1,02E-09	10,8	4,50E-09
183	10	0,50	5,46E-08	8,46E-10	10,1	3,94E-09
215	10	0,75	4,65E-08	7,20E-10	9,6	3,52E-09
718	30	1,00	4,18E-08	6,47E-10	9,3	3,26E-09
246	10	0,75	4,07E-08	6,29E-10	9,2	3,20E-09
234	10	0,50	4,27E-08	6,62E-10	9,3	3,31E-09
210	10	0,40	4,76E-08	7,37E-10	9,7	3,58E-09
259	10	1,00	3,86E-08	5,98E-10	9,0	3,08E-09
277	10	1,25	3,61E-08	5,59E-10	8,8	2,94E-09
295	10	1,50	3,39E-08	5,25E-10	8,6	2,81E-09
296	10	1,00	3,38E-08	5,23E-10	8,6	2,80E-09
248	10	0,40	4,03E-08	6,24E-10	9,2	3,18E-09
296	10	1,0	3,38E-08	5,23E-10	8,6	2,80E-09
337	10	1,50	2,97E-08	4,59E-10	8,3	2,56E-09
373	10	2,00	2,68E-08	4,15E-10	8,0	2,38E-09
346	10	1,00	2,89E-08	4,48E-10	8,2	2,51E-09
262	10	0,40	3,82E-08	5,91E-10	9,0	3,06E-09
318	10	1,00	3,14E-08	4,87E-10	8,4	2,66E-09
351	10	2,00	2,85E-08	4,41E-10	8,2	2,48E-09
380	10	2,50	2,63E-08	4,07E-10	7,9	2,35E-09
351	10	1,00	2,85E-08	4,41E-10	8,2	2,48E-09
281	10	0,40	3,56E-08	5,51E-10	8,8	2,91E-09

Coupling between changes in hydraulic and mechanical aperture*-Laboratory experiment*

20110301

Johan Thörn, PhD student, Division of GeoEngineering, Chalmers University of Technology

Flow/time calculations:

Time [s]	Volume [ml]	p cell [bar]	Time [s]	Volume [ml]	p cell [bar]
297	20	4	284	10	10
306	20	4	293	10	10
152	10	4	296	10	10
176	10	5	465	10	15
178	10	5	337	10	15
183	10	5	301	10	15
215	10	7,5	364	10	20
215	10	7,5	335	10	20
220	10	7,5	373	10	20
446	20	10	329	10	10
718	30	10	346	10	10
		10	331	10	10
247	10	7,5	267	10	4
244	10	7,5	260	10	4
246	10	7,5	262	10	4
237	10	5	311	10	10
233	10	5	317	10	10
234	10	5	318	10	10
209	10	4	339	10	20
208	10	4	345	10	20
210	10	4	351	10	20
245	10	10	370	10	25
258	10	10	373	10	25
259	10	10	380	10	25
272	10	12,5	350	10	10
272	10	12,5	349	10	10
277	10	12,5	351	10	10
291	10	15	305	10	4
278	10	15	282	10	4
295	10	15	281	10	4
291	10	10			
295	10	10			
296	10	10			
249	10	4	<i>The third time-value for each</i>		
244	10	4	<i>step has been used for further</i>		
248	10	4	<i>analysis.</i>		

Coupling between changes in hydraulic and mechanical aperture*-Laboratory experiment*

20110301

Johan Thörn, PhD student, Division of GeoEngineering, Chalmers University of Technology

Apertures:

p [MPa]	b [μm]	Δb [μm]	a [μm]	Δa [μm]	Δa/Δb [-]	Δa/Δb incr [-]
0,4	11	-	-	-	-	-
0,5	10	0,6	-	0,3	0,46	0,46
0,75	10	0,5	-	3,0	5,66	5,66
1	9	0,3	-	2,7	8,01	8,01
0,75	9	0,1	-	-0,8	-9,47	
0,5	9	-0,2	-	-2,2	14,26	
0,4	10	-0,3	-	-1,0	2,92	
1	9	0,7	-	4,7	7,19	7,19
1,25	9	0,2	-	2,2	11,01	11,01
1,5	9	0,2	-	2,6	14,19	14,19
1	9	0,0	-	-2,4	-246,37	
0,4	9	-0,5	-	-6,4	12,21	
1	9	0,5	-	4,5	8,58	8,58
1,5	8	0,4	-	4,0	10,95	10,95
2	8	0,3	-	4,1	14,91	14,91
1	8	-0,2	-	-5,6	27,63	
0,4	9	-0,8	-	-6,7	8,42	
1	8	0,6	-	4,8	8,54	8,54
2	8	0,3	-	7,4	27,12	27,12
2,5	8	0,2	-	3,2	15,03	15,03
1	8	-0,2	-	-8,4	39,45	
0,4	9	-0,6	-	-6,8	10,84	

Equations:

$$Q = \frac{V}{t}$$

$$S = 0,0109 \cdot T^{0,71}$$

$$T = \frac{Q \cdot L}{W \cdot dh}$$

$$k_n^S = \frac{\rho_w \cdot g}{S}$$

$$b = \sqrt[3]{\frac{12 \cdot \mu_w \cdot T}{\rho_w \cdot g}}$$

Coupling between changes in hydraulic and mechanical aperture

-Laboratory experiment

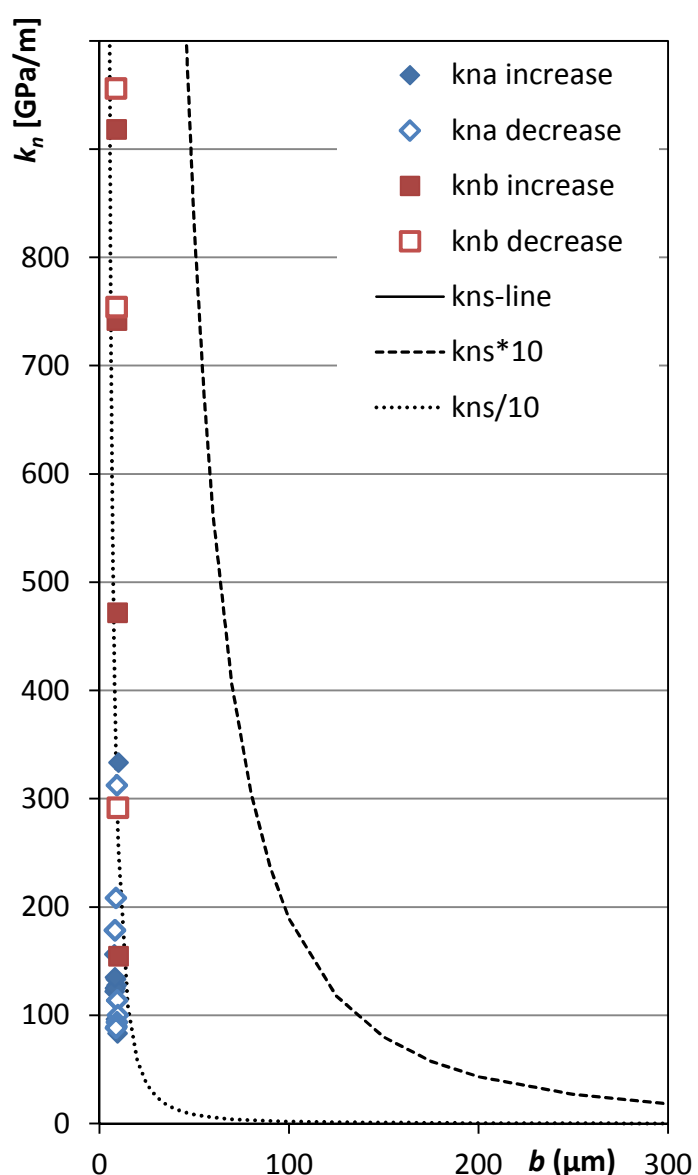
20110301

Johan Thörn, PhD student, Division of GeoEngineering, Chalmers University of Technology

Stiffness:

k_n^a ($\Delta\sigma'/\Delta a$) [GPa/m]	k_n^b ($\Delta\sigma'/\Delta b$) [GPa/m]	k_n^s 2176,5
333,3	154,7	2483,1
83,3	471,8	2784,1
92,6	741,6	3004,3
312,5	-2960,1	3063,5
113,6	1620,1	2956,6
100,0	291,7	2738,0
127,7	918,3	3177,6
113,6	1250,9	3332,8
96,2	1364,3	3485,2
208,3	-51327	3493,6
93,8	1144,3	3081,1
133,3	1144,3	3493,6
125,0	1368,9	3830,6
122,0	1818,4	4116,8
178,6	4934,2	3903,0
89,6	753,9	3203,6
125,0	1067,5	3676,0
135,1	3665,2	3942,9
156,3	2348,0	4171,5
178,6	7044,0	3942,9
88,2	956,1	3366,9

increase-steps in **bold**



Coupling between changes in hydraulic and mechanical aperture

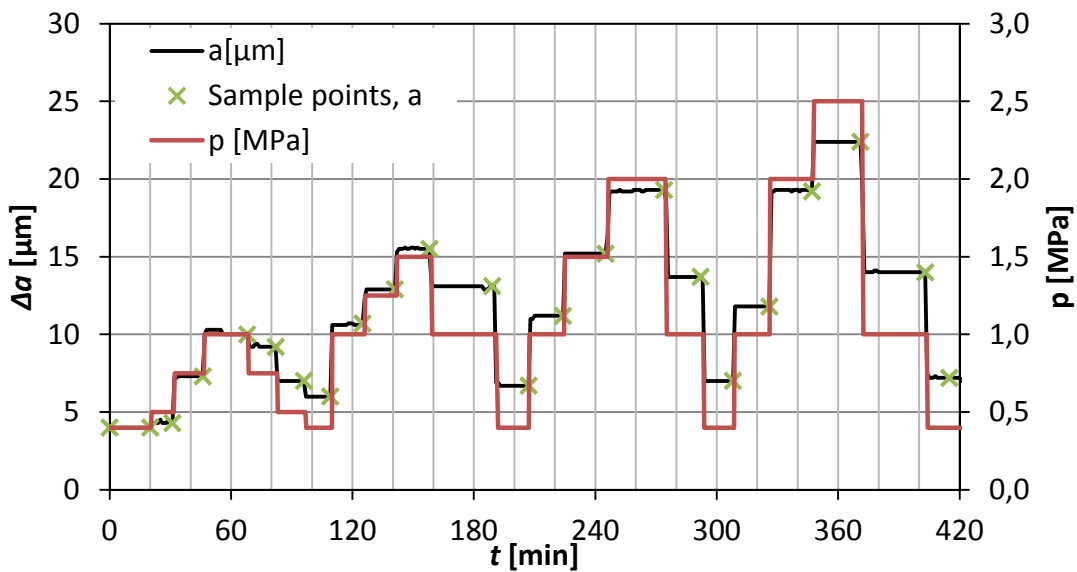
-Laboratory experiment

20110301

Johan Thörn, PhD student, Division of GeoEngineering, Chalmers University of Technology

Physical deformation:

<i>t</i> [min]	<i>a</i> [μm]	<i>p</i> [MPa]	Δa [μm]
20	4,0	0,4	0
31	4,3	0,5	0,3
46	7,3	0,75	3,0
68	10,0	1	2,7
82	9,2	0,75	-0,8
96	7,0	0,5	-2,2
109	6,0	0,4	-1,0
125	10,7	1	4,7
141	12,9	1,25	2,2
158	15,5	1,5	2,6
189	13,1	1	-2,4
207	6,7	0,4	-6,4
224	11,2	1	4,5
245	15,2	1,5	4,0
274	19,3	2	4,1
292	13,7	1	-5,6
308	7,0	0,4	-6,7
326	11,8	1	4,8
347	19,2	2	7,4
371	22,4	2,5	3,2
403	14,0	1	-8,4
415	7,2	2	-6,8



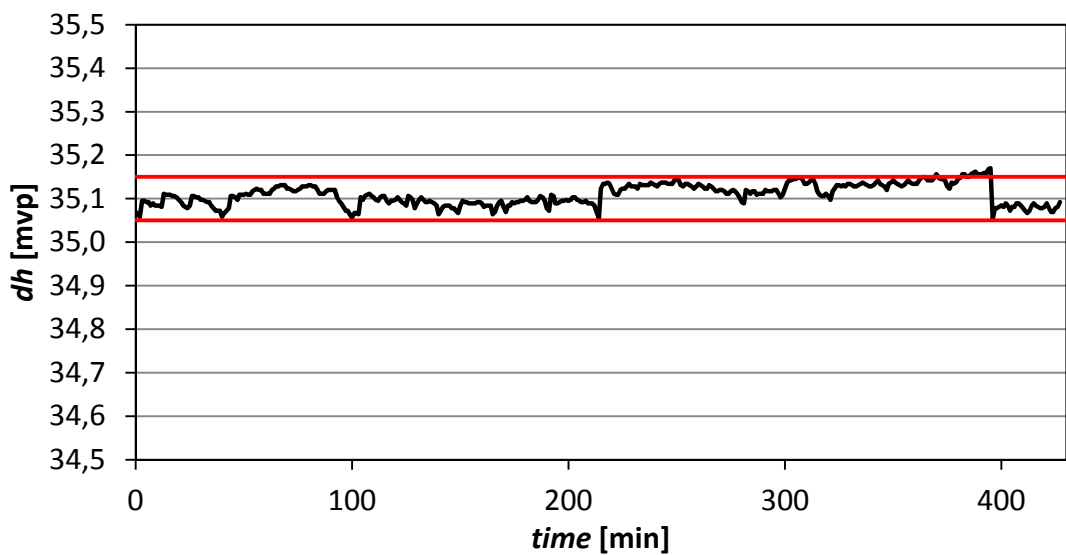
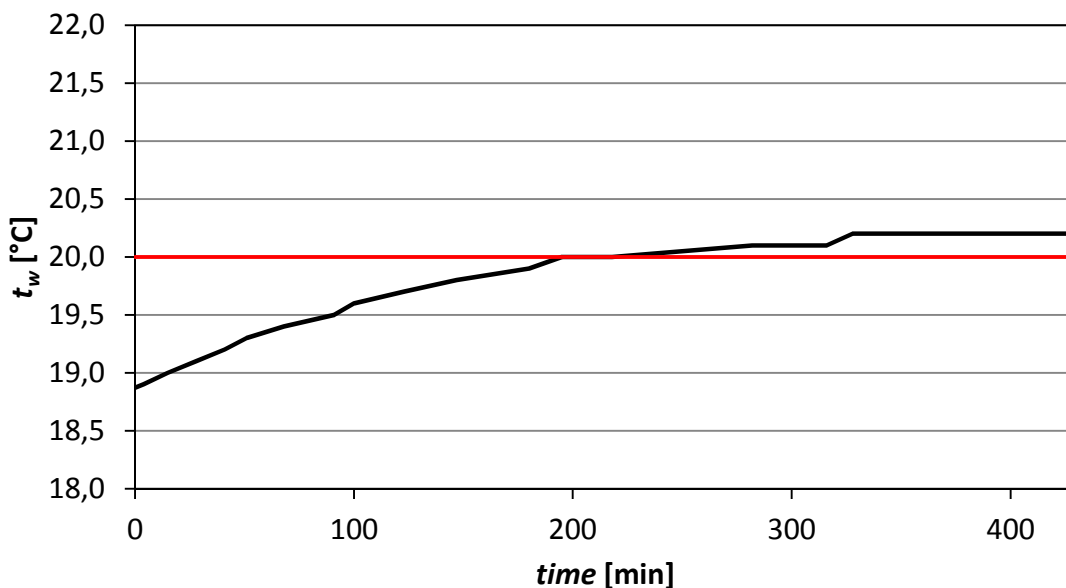
Coupling between changes in hydraulic and mechanical aperture*-Laboratory experiment*

20110301

Johan Thörn, PhD student, Division of GeoEngineering, Chalmers University of Technology

***dh* reliability:**

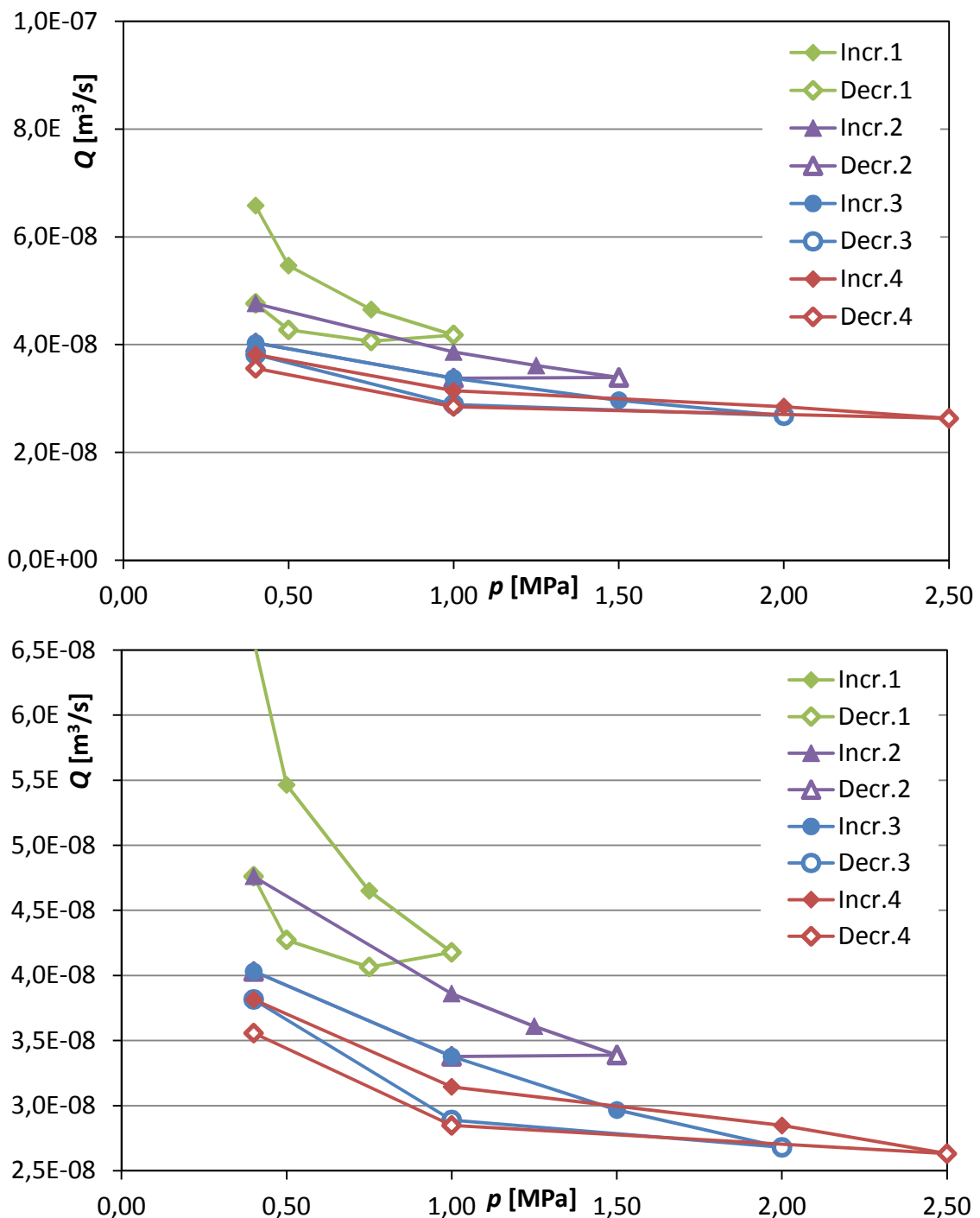
Set value	35,1 m	set value ± 5 cm	95,68%
no. Sec. < 35,05	12 s	0,05%	
no. Sec. >35,15	1098 s	4,28%	
total time	25672 s		
mean	35,109557 m		
stdev	0,0242556 m		

***t_w* reliability:**

Coupling between changes in hydraulic and mechanical aperture*-Laboratory experiment*

20110301

Johan Thörn, PhD student, Division of GeoEngineering, Chalmers University of Technology

Flow-pressure graphs

$$\begin{aligned} T &= 20^\circ\text{C} \\ \rho_f &= 998,2071 \text{ kg/m}^3 \\ g &= 9,81 \text{ m/s}^2 \\ C_f &= 4,59\text{E-}10 \text{ Pa}^{-1} \end{aligned}$$

$$S1 = \rho_f g \left(\frac{1}{k_n} + e C_f \right)$$

$$S2 = \rho_f g \left(\frac{1}{k_n} \right)$$

$$diff = \frac{S1 - S2}{S1}$$

Fine RA, Millero FJ (1973) Compressibility of water as a function of temperature and pressure. The Journal of Chemical Physics 59 (5529). doi:<http://dx.doi.org/10.1063/1.1679903>

Approximate range of experimental results

Diff Kn (GPa/m)	e (μm)	5	10	20	30	40	50	60	70	80	90	100	120	140	160	180	200	250	300
1,0	0,0%	0,0%	0,0%	0,0%	0,0%	0,0%	0,0%	0,0%	0,0%	0,0%	0,0%	0,0%	0,0%	0,0%	0,0%	0,0%	0,0%	0,0%	0,0%
1,4	0,0%	0,0%	0,0%	0,0%	0,0%	0,0%	0,0%	0,0%	0,0%	0,0%	0,0%	0,0%	0,0%	0,0%	0,0%	0,0%	0,0%	0,0%	0,0%
2,0	0,0%	0,0%	0,0%	0,0%	0,0%	0,0%	0,0%	0,0%	0,0%	0,0%	0,0%	0,0%	0,0%	0,0%	0,0%	0,0%	0,0%	0,0%	0,0%
2,8	0,0%	0,0%	0,0%	0,0%	0,0%	0,0%	0,0%	0,0%	0,0%	0,0%	0,0%	0,0%	0,0%	0,0%	0,0%	0,0%	0,0%	0,0%	0,0%
4,0	0,0%	0,0%	0,0%	0,0%	0,0%	0,0%	0,0%	0,0%	0,0%	0,0%	0,0%	0,0%	0,0%	0,0%	0,0%	0,0%	0,0%	0,0%	0,1%
5,6	0,0%	0,0%	0,0%	0,0%	0,0%	0,0%	0,0%	0,0%	0,0%	0,0%	0,0%	0,0%	0,0%	0,0%	0,0%	0,0%	0,0%	0,1%	0,1%
7,9	0,0%	0,0%	0,0%	0,0%	0,0%	0,0%	0,0%	0,0%	0,0%	0,0%	0,0%	0,0%	0,0%	0,0%	0,0%	0,0%	0,1%	0,1%	0,1%
11,2	0,0%	0,0%	0,0%	0,0%	0,0%	0,0%	0,0%	0,0%	0,0%	0,0%	0,0%	0,0%	0,0%	0,0%	0,0%	0,0%	0,1%	0,1%	0,2%
15,8	0,0%	0,0%	0,0%	0,0%	0,0%	0,0%	0,0%	0,0%	0,0%	0,0%	0,1%	0,1%	0,1%	0,1%	0,1%	0,1%	0,1%	0,2%	0,2%
22,4	0,0%	0,0%	0,0%	0,0%	0,0%	0,0%	0,0%	0,1%	0,1%	0,1%	0,1%	0,1%	0,1%	0,1%	0,1%	0,2%	0,2%	0,3%	0,3%
31,6	0,0%	0,0%	0,0%	0,0%	0,0%	0,0%	0,1%	0,1%	0,1%	0,1%	0,1%	0,1%	0,1%	0,2%	0,2%	0,2%	0,3%	0,4%	0,4%
44,7	0,0%	0,0%	0,0%	0,0%	0,1%	0,1%	0,1%	0,1%	0,1%	0,1%	0,1%	0,1%	0,2%	0,2%	0,2%	0,3%	0,4%	0,5%	0,6%
63,1	0,0%	0,0%	0,1%	0,1%	0,1%	0,1%	0,1%	0,2%	0,2%	0,2%	0,2%	0,3%	0,3%	0,3%	0,3%	0,5%	0,5%	0,6%	0,9%
89,1	0,0%	0,0%	0,1%	0,1%	0,1%	0,2%	0,2%	0,2%	0,3%	0,3%	0,4%	0,4%	0,4%	0,5%	0,6%	0,7%	0,7%	0,8%	1,0%
125,9	0,0%	0,1%	0,1%	0,2%	0,2%	0,2%	0,3%	0,3%	0,4%	0,4%	0,5%	0,5%	0,6%	0,7%	0,8%	0,9%	1,0%	1,1%	1,4%
177,8	0,0%	0,1%	0,2%	0,2%	0,3%	0,3%	0,4%	0,5%	0,6%	0,6%	0,7%	0,8%	1,0%	1,1%	1,1%	1,3%	1,4%	1,6%	2,4%
251,2	0,1%	0,1%	0,2%	0,3%	0,5%	0,6%	0,7%	0,8%	0,9%	1,0%	1,0%	1,1%	1,4%	1,6%	1,8%	2,0%	2,3%	2,8%	3,3%
354,8	0,1%	0,2%	0,3%	0,5%	0,6%	0,8%	1,0%	1,1%	1,3%	1,4%	1,6%	1,9%	2,2%	2,2%	2,5%	2,8%	3,2%	3,9%	4,7%
501,2	0,1%	0,2%	0,5%	0,7%	0,9%	1,1%	1,4%	1,6%	1,8%	2,0%	2,2%	2,7%	3,1%	3,5%	4,0%	4,4%	5,4%	6,5%	
707,9	0,2%	0,3%	0,6%	1,0%	1,3%	1,6%	1,9%	2,2%	2,5%	2,8%	3,1%	3,8%	4,4%	4,9%	5,5%	6,1%	7,5%	8,9%	
1000,0	0,2%	0,5%	0,9%	1,4%	1,8%	2,2%	2,7%	3,1%	3,5%	4,0%	4,4%	5,2%	6,0%	6,8%	7,6%	8,4%	10,3%	12,1%	
1412,5	0,3%	0,6%	1,3%	1,9%	2,5%	3,1%	3,7%	4,3%	4,9%	5,5%	6,1%	7,2%	8,3%	9,4%	10,4%	11,5%	13,9%	16,3%	
1995,3	0,5%	0,9%	1,8%	2,7%	3,5%	4,4%	5,2%	6,0%	6,8%	7,6%	8,4%	9,9%	11,4%	12,8%	14,2%	15,5%	18,6%	21,6%	
2818,4	0,6%	1,3%	2,5%	3,7%	4,9%	6,1%	7,2%	8,3%	9,4%	10,4%	11,5%	13,4%	15,3%	17,1%	18,9%	20,6%	24,4%	28,0%	
3981,1	0,9%	1,8%	3,5%	5,2%	6,8%	8,4%	9,9%	11,3%	12,8%	14,1%	15,4%	18,0%	20,4%	22,6%	24,7%	26,8%	31,4%	35,4%	
5623,4	1,3%	2,5%	4,9%	7,2%	9,4%	11,4%	13,4%	15,3%	17,1%	18,8%	20,5%	23,6%	26,5%	29,2%	31,7%	34,0%	39,2%	43,6%	
7933,3	1,8%	3,5%	6,8%	9,9%	12,7%	15,4%	17,9%	20,3%	22,6%	24,7%	26,7%	30,4%	33,8%	36,8%	39,6%	42,2%	47,7%	52,2%	
11220,2	2,5%	4,9%	9,3%	13,4%	17,1%	20,5%	23,6%	26,5%	29,2%	31,7%	34,0%	38,2%	41,9%	45,2%	48,1%	50,7%	56,3%	60,7%	

Appendix XI. Note on uncertainties

Note

Coupling between changes in hydraulic and mechanical aperture

-A laboratory study on rock cores

--Uncertainty estimates of measured and calculated data

Johan Thörn, PhD student, Division of GeoEngineering, Chalmers University of Technology

Written as a part of Graduate course Probabilistic Risk Assessment (PRA), spring 2011



1 Table of contents

1	Table of contents	1
2	Introduction	1
3	Building the uncertainty model.....	2
3.1	Variables	2
4	Results.....	5
5	Conclusions.....	7
5.1	Further work.....	7
Appendix A.	Statistics from Crystal ball simulation.....	8
Appendix B.	Percentiles from Crystal ball simulation	9
Appendix C.	Sensitivity data from Crystal ball simulation	10
Appendix D.	Sketch of test setup and identified uncertainties.....	11
Appendix E.	Crystal ball model	12

2 Introduction

This note describes the efforts of estimating the uncertainty of laboratory experiments performed on rock cores. A thorough description of the experiments is carried out in the main report “**Coupling between changes in hydraulic and mechanical aperture –A laboratory study on rock cores**”.

The work is carried out as a course project in the graduate course “Probabilistic Risk Assessment (PRA)”, given at the department of Civil and Environmental Engineering, Chalmers University of Technology, during spring and summer 2011.

Uncertainty calculations have been made for the hydraulic testing with simultaneous deformation measurements of the core AB1AB2. The analysis can be expanded to include data from the other tested cores within this project. The software used is Crystal Ball from Oracle, which is a plug-in program for Microsoft Excel.

The primary objective is testing the $\Delta a/\Delta b$ -ratio, which is an output of the experiments. An expansion to other test results, such as fracture stiffness evaluations is possible.

3 Building the uncertainty model

The experimental setup was analysed with regard to possible sources of measurement error and conceptual errors. These errors were categorized according to which part of the setup they belonged to. The results are presented in Appendix D, and are summarized in Table 1. In Crystal Ball, Excel calculations are carried out in a regular fashion, but cells can be given distributions; *Assumption*, rather than point values. A run of the program renders 100 000 calculations, with random values according to the chosen distribution. Other cells can be marked as *Forecasts*, from which a set of statistical data is available after the simulation run. Such data is presented in Appendix A and Appendix B. A graphical representation of sensitivity to different variables (denoted *Assumption* in Crystal Ball) gets available, Figure 4.

3.1 Variables

The path for calculations from the experimental results is presented in Figure 1. The variables to the right is measured during or before the experiment, and each associated with one or more uncertainties, as specified in Table 1. The Monte Carlo-simulation run by Crystal ball renders a distribution of the variability associated with $\Delta a/\Delta b$. The simulation is run 100 000 iterations, which gives a stable output.

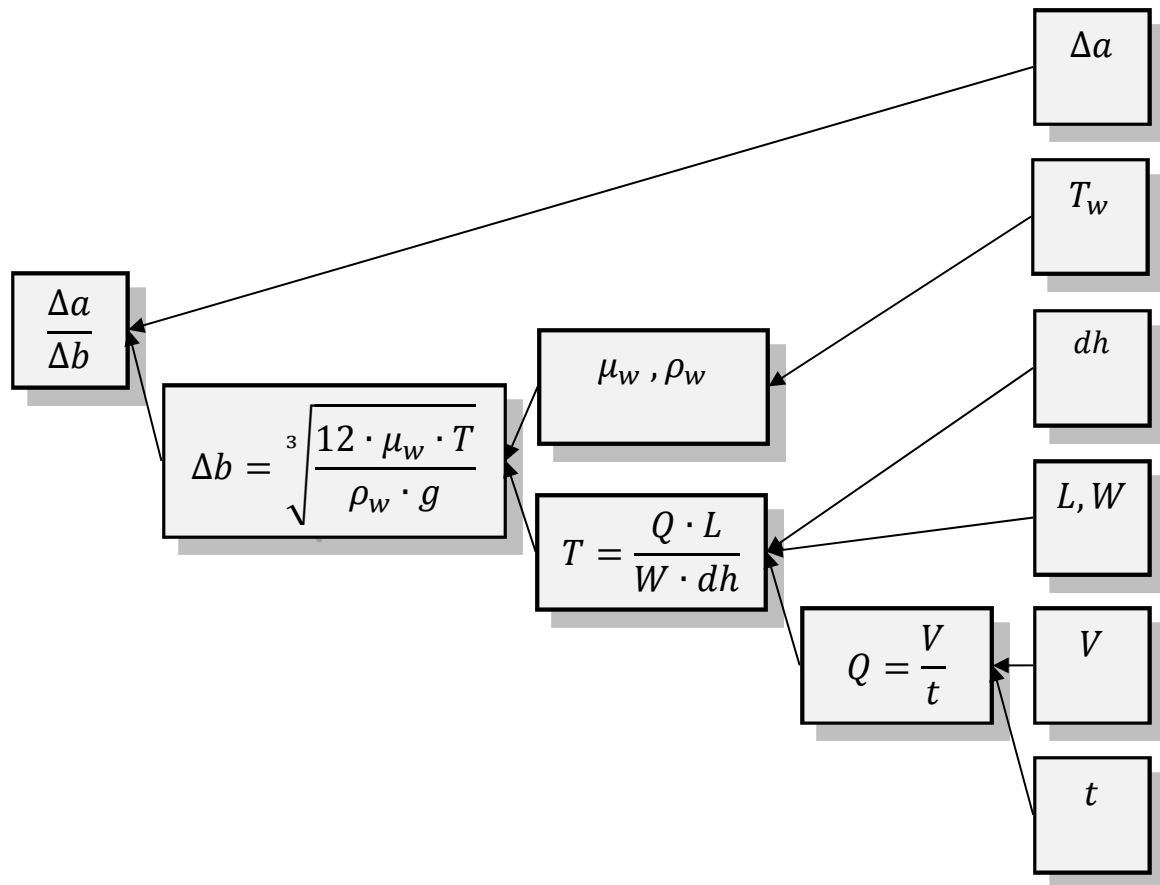


Figure 1: Calculation flowchart. The variables to the right are measured in some way during or before the experiment.

In Table 1, the variable distributions are color coded, with green for measured, or quite certain assumptions. Yellow is used for more vague assumptions. All assumptions but one are same for all pressure steps, and the last one is given one value for each pressure step. This value is calculated by plotting points of finished flow measurements on a time scale starting from when the pressure step was achieved (Figure 2) and interpolating the points. The time for when the corresponding physical deformation value has been constant for a threshold of 5 min is used for determining a fixed point on the interpolated line. The deviation between “interpolated flow/stable deformation”-value and the third flow measurement is calculated as a percentage. The largest of this percentage or 2% is used as standard deviation as well as addition to the third flow reading; giving a mean value in the Crystal ball *assumptions*.

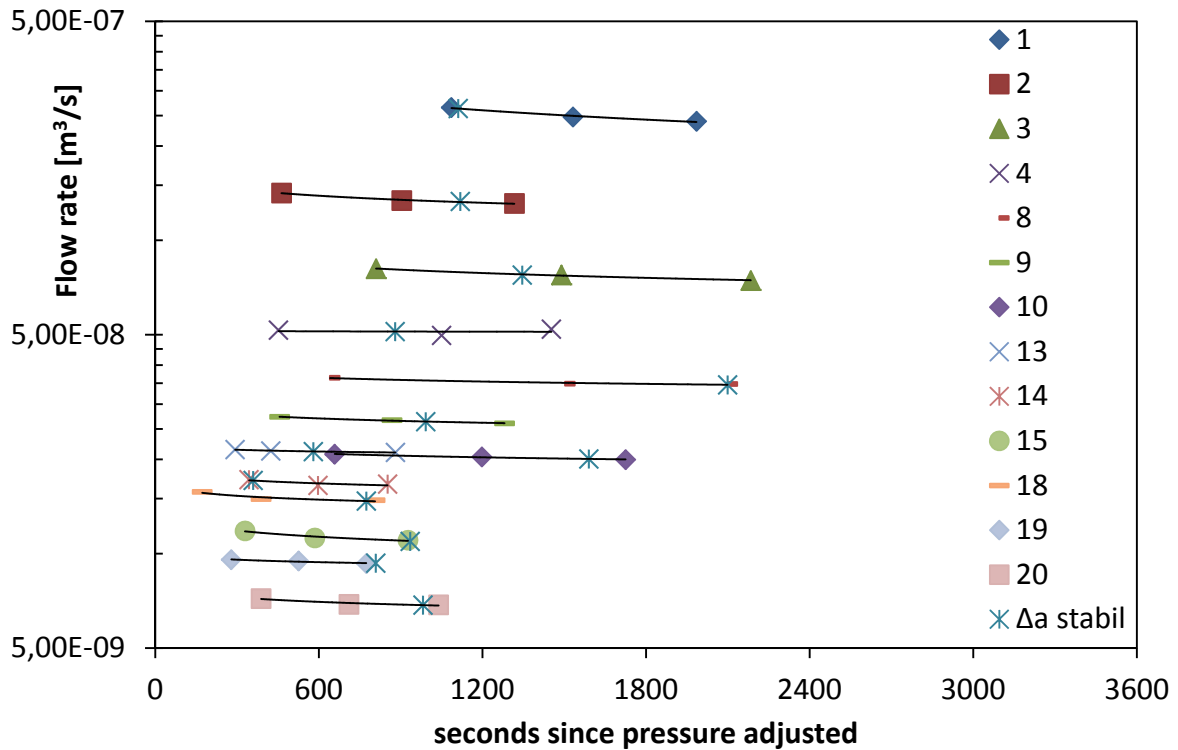


Figure 2: Defining the relation between flow time for third measurement and the point where deformation had been stable for 5 minutes. Data only shown for increase-pressure steps.

Table 1: Uncertainty variables identified in the experimental setup. The type of variable is chosen between *Conceptual*, *Assessable Measurable* or *Measured*. The assigned value is a distribution, *measured*, *Insignificant*, *robust* or *Not regarded*. Values that are measured or, by personal judgment regarded as stable are marked green, less confident values are yellow.

Category	Type	Assigned value
Variable		
Conceptual for entire test		
· p valid as normal stress	Conceptual	Not regarded
· Δa representative as normal deformation	Conceptual	Not regarded
· Scale effects	Conceptual	Not regarded
· Cubic law valid	Conceptual	Robust
Test water		
· De-aeration sufficient	Assessable	TBA N(for each value)
p measurements and regulation		
· Accuracy manometer	Measured	$N(0; 2\%)^2$
dh measurement and regulation		
· Accuracy pressure sensor		$N(0; 1\%)^2$
· Calibration pressure sensor		$N(0; 1\%)^2$
· Accuracy logger		$N(0; 1\%)^2$
· Friction losses in system	Assessable	Insignificant
· dh	Measured	$\sigma=0.006 \mu=0.64$
Fracture sample		
· W representative as width of fracture	Conceptual	Robust
· Accuracy determination W	Measurable	$N(0; 2\%)^2$
· L representative as length of fracture	Conceptual	Robust
· Accuracy determination L	Measurable	$N(0; 2\%)^2$
Physical deformation measurements		
· Accuracy LVDT		$N(0; 2\%)^2$
· Accuracy logger		$N(0; 1\%)^2$
· Stability glued brackets	Assessable	Robust
Water temperature measurements		
· Accuracy thermometer	Measurable	$N(0; 0.5^\circ C)^2$
· Overflow water representative for sample	Assessable	$N(0; 0.2^\circ C)^2$
· Temperature variation with time	Measured	$\sigma=0.3^\circ \mu=20.3^\circ$
Flow measurements		
· Tolerance measurement cylinder	Assessable	$N(0; 1\%)^2$
· Reading technique measurement cylinder	Assessable	$N(0; 2\%)^2$
· Round-off time to whole second	Assessable	$U(0; 1)$
· Delay reading-time stamp		$N(+0.5; 0.5^2)$
· Unsteady flow past overflow Mainly eliminated through triple measurements and discrimination of deviating values.	Assessable	
· Leakage of cell water into test water (Cell water dyed)	Measured	$T= 3 \cdot 10^{-12} m^2/s$ Insignificant

4 Results

In Figure 3, the data points of all pressure steps for the testing of core AB1AB2 are plotted as $\Delta a/\Delta b$ -ratio against b . The error bars presented for each point represents the 20% and 80% percentiles. It is clear that the results are quite precise for the increase-pressure values (filled blue) and more uncertain for the reduce-pressure values (unfilled blue).

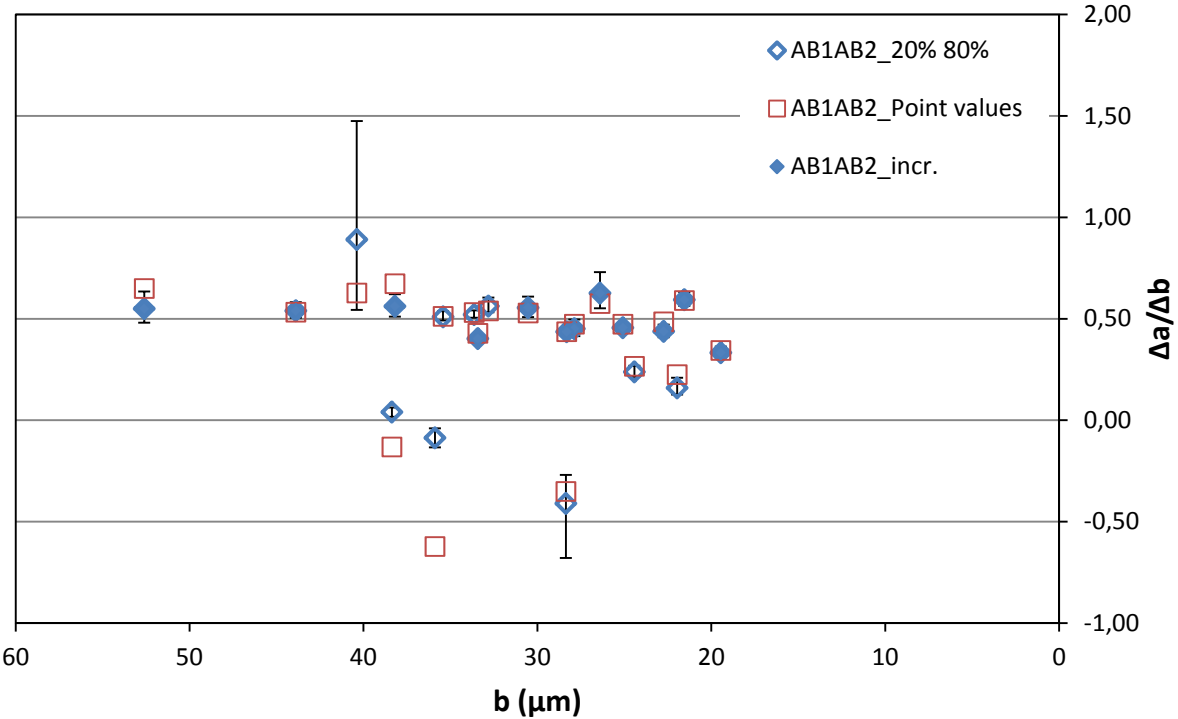


Figure 3: Hydraulic aperture (b) plotted against $\Delta a/\Delta b$ -ratio for all pressure steps of AB1AB2 test. The error bars represent 20% and 80%-percentiles. Evaluated with Crystal Ball.

The effect that each uncertain variable has on the total variance of the output is displayed for one pressure step in Figure 4. The other steps are similar, with few exceptions; for some steps the LVDT-value gets larger than one of the time readings.

Step19

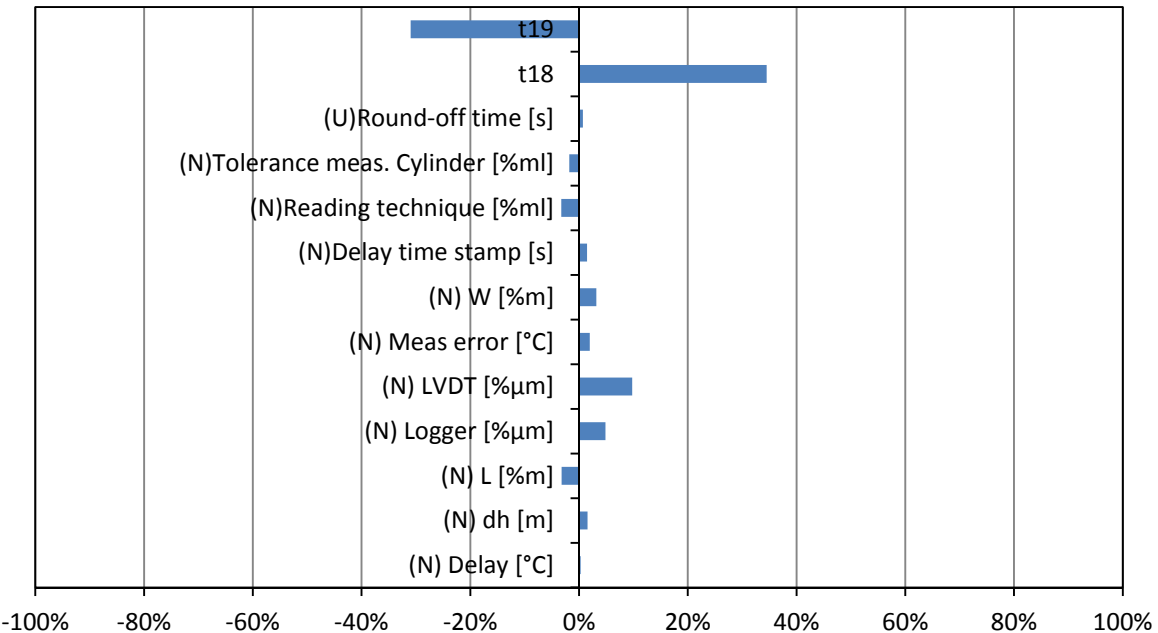


Figure 4: Sensitivity chart for one data point from AB1AB2 (the increase from 2-2.5 MPa). Sensitivity is expressed as the contribution to total variance. t18 and t19 are values assigned for the flow time, which is set as a normal distribution with μ and σ equal to the difference between time for the third flow measurement and the point where deformation value has been stable for 5 minutes

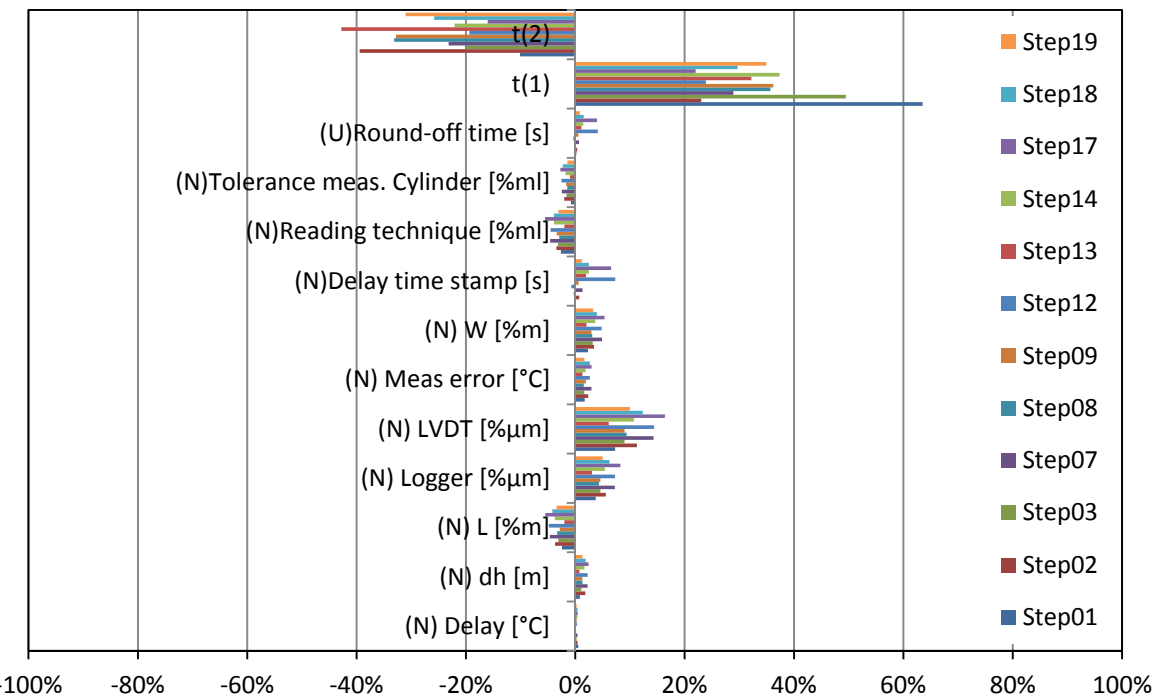


Figure 5: Sensitivity chart for all increase-pressure steps. Data for all of the pressure steps are presented in a table in Appendix C.

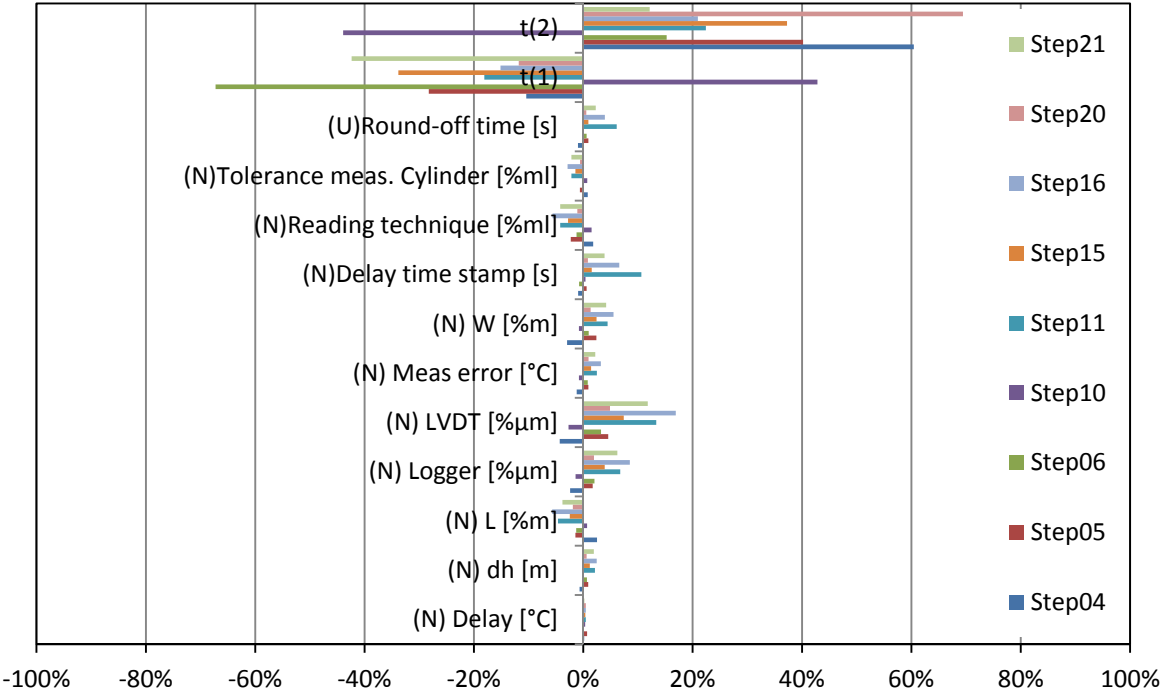


Figure 6: Sensitivity chart for all decrease-pressure steps. Data for all of the pressure steps are presented in a table in Appendix C.

5 Conclusions

The simulations show a good agreement between the “increasing pressure steps” and the point values from previous analysis. For the “decreasing pressure steps” the agreement is not as good, and more effort is needed to understand these, if the decrease-pressure steps are to be used in the same way as the increase-pressure steps. The variability of the results mainly originates from the estimates of representative time for flow measurements.

5.1 Further work

The value with the biggest impact on the results would be interesting to examine further. Therefore a simple comparing test is set up for determining the effect of de-aeration of water on the flow rate with time. For the experiments presented above, a de-aeration of three hours was used. A single low pressure step, held for a day with periodic flow measurements might be able to indicate differences between a more thoroughly de-aerated sample and container and the de-aeration procedure used in the experiments.

Further, an expansion of the crystal ball model to include fracture stiffness is desired, as well as running the simulation for the other two tested samples.

Appendix A. Statistics from Crystal ball simulation

Statistics, 100000 trials	Base Case	Mean	Median	Standard Deviation	Variance	Skewness	Kurtosis	Coeff. of Variability	Minimum	Maximum	Range Width	Mean Std. Error
Step01	0,55	0,56	0,55	0,096	0,0092	0,66	3,9	0,17	0,29	1,3	1	0,0003
Step02	0,54	0,54	0,54	0,047	0,0022	0,58	3,7	0,086	0,4	0,85	0,44	0,00015
Step03	0,56	0,57	0,56	0,068	0,0046	0,59	3,8	0,12	0,36	1,1	0,74	0,00021
Step04	-0,087	-2,4	-0,067	720	510000	-320	1000000	-300	-230000	3400	230000	2,3
Step05	0,04	0,31	0,03	110	13000	300	95000	360	-4800	35000	40000	0,35
Step06	0,89	0,76	0,81	160	26000	-130	47000	210	-41000	24000	65000	0,51
Step07	0,4	0,4	0,4	0,023	0,00053	0,26	3,1	0,057	0,31	0,52	0,21	0,000073
Step08	0,55	0,56	0,55	0,062	0,0039	0,66	3,9	0,11	0,38	0,98	0,6	0,0002
Step09	0,45	0,46	0,45	0,051	0,0026	0,68	4	0,11	0,31	0,88	0,57	0,00016
Step10	-0,41	-0,68	-0,39	32	1100	-190	45000	-48	-8300	1400	9700	0,1
Step11	0,51	0,52	0,51	0,027	0,00076	0,23	3,1	0,053	0,41	0,66	0,25	0,000087
Step12	0,44	0,44	0,44	0,022	0,00051	0,22	3,1	0,051	0,35	0,56	0,21	0,000071
Step13	0,63	0,65	0,63	0,12	0,014	2,1	42	0,19	0,37	5,9	5,5	0,00038
Step14	0,44	0,44	0,44	0,038	0,0014	0,42	3,4	0,085	0,31	0,67	0,35	0,00012
Step15	0,24	0,24	0,24	0,035	0,0012	0,89	4,7	0,14	0,15	0,53	0,38	0,00011
Step16	0,52	0,52	0,52	0,021	0,00046	0,13	3	0,041	0,44	0,64	0,2	0,000068
Step17	0,46	0,46	0,46	0,02	0,00038	0,14	3	0,043	0,38	0,55	0,16	0,000062
Step18	0,59	0,6	0,6	0,041	0,0017	0,33	3,2	0,068	0,46	0,86	0,4	0,00013
Step19	0,33	0,34	0,33	0,033	0,0011	0,54	3,6	0,098	0,23	0,53	0,3	0,0001
Step20	0,16	0,17	0,16	0,085	0,0072	-38	6200	0,49	-13	5	18	0,00027
Step21	0,56	0,57	0,56	0,046	0,0021	0,82	4,6	0,081	0,43	1	0,61	0,00015

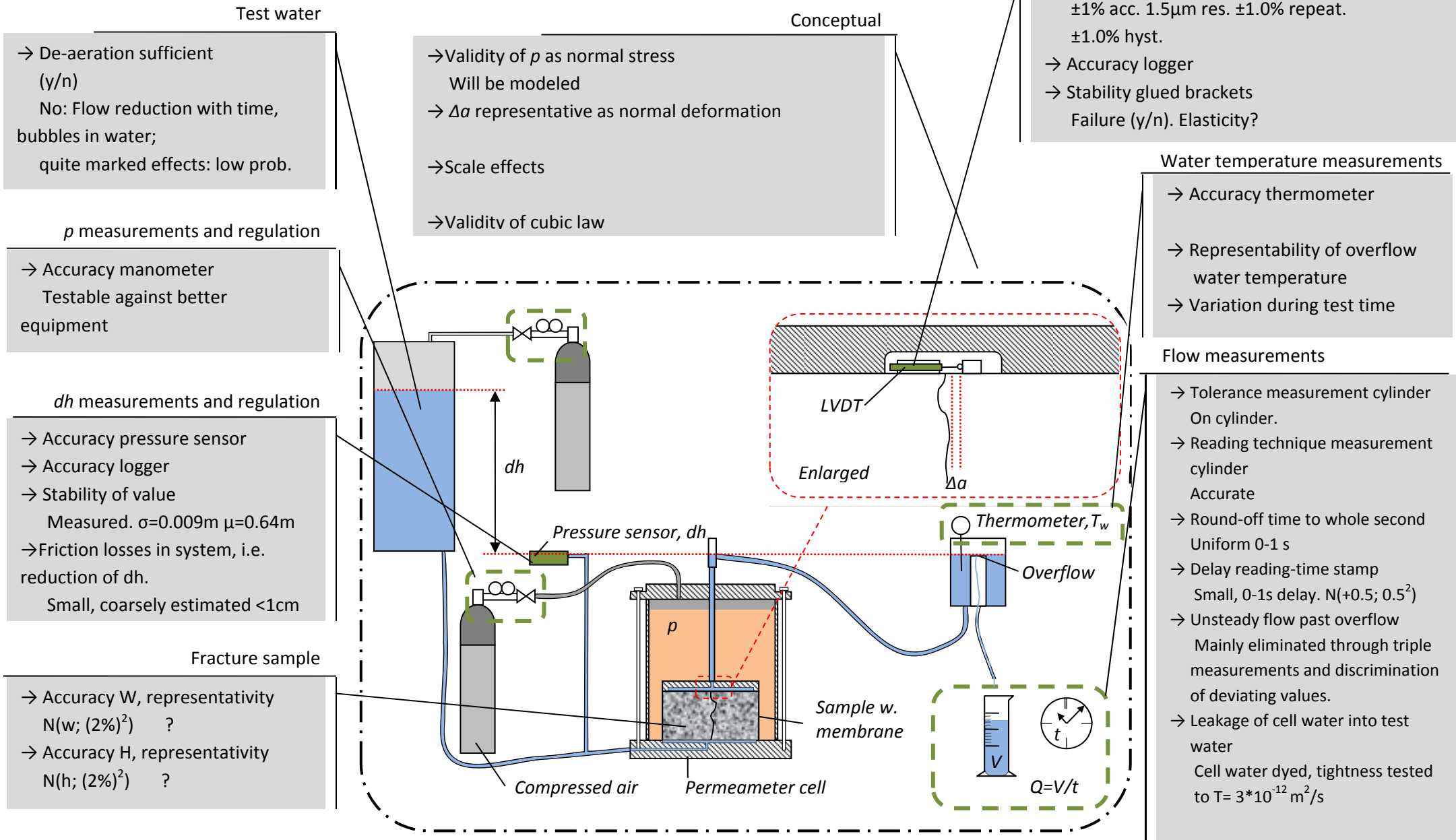
Appendix B. Percentiles from Crystal ball simulation

Percentiles	0%	10%	20%	30%	40%	50%	60%	70%	80%	90%	100%
Step01	0,29	0,45	0,48	0,5	0,53	0,55	0,57	0,6	0,64	0,69	1,3
Step02	0,4	0,49	0,51	0,52	0,53	0,54	0,55	0,57	0,58	0,61	0,85
Step03	0,36	0,49	0,51	0,53	0,55	0,56	0,58	0,6	0,62	0,66	1,1
Step04	-230000	-0,23	-0,13	-0,099	-0,08	-0,067	-0,057	-0,049	-0,04	0,12	3400
Step05	-4800	-0,062	0,016	0,021	0,025	0,03	0,036	0,046	0,063	0,11	35000
Step06	-41000	0,44	0,54	0,62	0,71	0,81	0,94	1,1	1,5	2,4	24000
Step07	0,31	0,37	0,38	0,39	0,4	0,4	0,41	0,41	0,42	0,43	0,52
Step08	0,38	0,49	0,51	0,52	0,54	0,55	0,57	0,59	0,61	0,64	0,98
Step09	0,31	0,4	0,41	0,43	0,44	0,45	0,46	0,48	0,5	0,52	0,88
Step10	-8300	-1	-0,68	-0,54	-0,45	-0,39	-0,35	-0,31	-0,27	-0,23	1400
Step11	0,41	0,48	0,49	0,5	0,51	0,51	0,52	0,53	0,54	0,55	0,66
Step12	0,35	0,41	0,42	0,43	0,43	0,44	0,44	0,45	0,46	0,47	0,56
Step13	0,37	0,52	0,55	0,58	0,6	0,63	0,65	0,69	0,73	0,8	5,9
Step14	0,31	0,4	0,41	0,42	0,43	0,44	0,45	0,46	0,47	0,49	0,67
Step15	0,15	0,2	0,21	0,22	0,23	0,24	0,25	0,26	0,27	0,29	0,53
Step16	0,44	0,5	0,51	0,51	0,52	0,52	0,53	0,53	0,54	0,55	0,64
Step17	0,38	0,43	0,44	0,45	0,45	0,46	0,46	0,47	0,47	0,48	0,55
Step18	0,46	0,55	0,56	0,58	0,59	0,6	0,61	0,62	0,63	0,65	0,86
Step19	0,23	0,3	0,31	0,32	0,33	0,33	0,34	0,35	0,36	0,38	0,53
Step20	-13	0,11	0,13	0,14	0,15	0,16	0,17	0,19	0,21	0,25	5
Step21	0,43	0,52	0,53	0,54	0,55	0,56	0,58	0,59	0,6	0,63	1

Appendix C. Sensitivity data from Crystal ball simulation

	Sensitivity Data											
	(U)Round-off time [s]											
	(N)Tolerance meas. Cylinder [%ml]											
	(N)Reading technique [%ml]											
	(N)Delay time stamp [s]											
	(N) W [%m]											
	(N) Meas error [°C]											
	(N) LVDT [%μm]											
	(N) Logger [%μm]											
	(N) L [%m]											
	(N) dh [m]											
	(N) Delay [°C]											
Step01	1%	-1%	-2%	4%	7%	2%	2%	0%	-3%	-1%	0%	64% -10%
Step02	0%	2%	-4%	6%	11%	2%	3%	1%	-3%	-2%	0%	23% -39%
Step03	0%	1%	-3%	5%	9%	2%	3%	0%	-3%	-2%	0%	49% -20%
Step04	0%	-1%	3%	-2%	-4%	-1%	-3%	-1%	2%	1%	-1%	-10% 60%
Step05	1%	1%	-1%	2%	5%	1%	2%	1%	-2%	-1%	1%	-28% 40%
Step06	0%	1%	-1%	2%	3%	1%	1%	-1%	-1%	0%	1%	-6% 15%
Step07	0%	2%	-5%	7%	14%	3%	5%	1%	-5%	-2%	1%	29% -23%
Step08	0%	1%	-3%	4%	9%	2%	3%	-1%	-3%	-1%	0%	36% -33%
Step09	0%	1%	-3%	5%	9%	2%	3%	1%	-3%	-2%	1%	36% -33%
Step10	0%	0%	1%	-1%	-3%	-1%	0%	0%	2%	1%	0%	43% -44%
Step11	0%	2%	-5%	7%	13%	2%	4%	11%	-4%	-2%	6%	-18% 22%
Step12	0%	2%	-5%	7%	14%	3%	5%	7%	-5%	-3%	4%	24% -19%
Step13	0%	1%	-2%	3%	6%	1%	2%	2%	-2%	-1%	1%	32% -43%
Step14	0%	2%	-4%	5%	11%	2%	4%	2%	-4%	-2%	1%	37% -22%
Step15	0%	1%	-2%	4%	7%	1%	2%	2%	-3%	-1%	1%	-34% 37%
Step16	0%	2%	-6%	9%	17%	3%	6%	7%	-6%	-3%	4%	-15% 21%
Step17	0%	2%	-5%	8%	16%	3%	5%	7%	-6%	-3%	4%	22% -16%
Step18	0%	2%	-4%	6%	12%	3%	4%	2%	-4%	-2%	2%	30% -26%
Step19	0%	1%	-3%	5%	10%	2%	3%	1%	-3%	-1%	1%	35% -31%
Step20	0%	1%	-2%	2%	5%	1%	1%	1%	-1%	-1%	1%	-12% 69%
Step21	0%	2%	-4%	6%	12%	2%	4%	4%	-4%	-2%	2%	-42% 12%

Appendix D. Sketch of test setup and identified uncertainties



Appendix E. Crystal ball model

AB1AB2		(N)Tolerance meas. Cylinder [%ml]				0	1%	(N) W [%m]	0,1925	0,00385 2%		Crystal ball assumption											
		(N)Reading technique [%ml]				0	2%	(N) L [%m]	0,104	0,00208 2%		Data extracted from Analysis sheet											
		(U)Round-off time [s]				0	1	(N) dh [m]	0,640665	0,00564 0,9%		Time for syncing of temperature to rest of data set											
(N) Logger [%μm]		0	1%	(U)Delay time stamp [s]				g [m/s2]	9,81	(N) Delay [°C]		0	0,2	Crystal Ball forecast									
(N) LVDT [%μm]		0	2%	(N)Delay time stamp [s]						(N) Meas error [°C]		0	0,5										
Time [min]		Δa	Δa _{adj}	t	μ	σ	t _{adj}	V	V _{adj}	Q	T	Time	T _w	T _{w adj}	μ _w	ρ _w	b	Δb	Δa/Δb	Δa/Δb	20%- perc. Δa/Δb	80%- perc. Δa/Δb	
[s]	[s]				[s]	[s]	[s]	[ml]	[ml]	[m ³ /s]	[m ² /s]	[min]	[°C]	[°C]	[Pas]	[kg/m ³]	[μm]	[μm]	[-]	[-]			
Step00				417	-38	37,6	380	100	100	2,63E-07	2,22E-07		39	20	20	1,06E-03	998,28	66					
Step01	46	7,4	7,4	381	-5	7,6	376	50	50	1,33E-07	1,12E-07		66	20	20	1,06E-03	998,28	53	13,5	0,55	0,65	0,48	0,64
Step02	84	4,7	4,7	672	-26	26,3	646	50	50	7,74E-08	6,53E-08		71	20,1	20,1	1,06E-03	998,26	44	8,7	0,54	0,53	0,51	0,58
Step03	111	3,2	3,2	384	7	7,7	391	20	20	5,11E-08	4,31E-08		99	20,2	20,2	1,06E-03	998,24	38	5,7	0,56	0,67	0,51	0,62
Step04	151	-0,2	-0,2	394	75	75,0	470	20	20	4,26E-08	3,59E-08		140	20,4	20,4	1,05E-03	998,20	36	2,3	-0,09	-0,62	-0,13	-0,04
Step05	189	-0,1	-0,1	419	-36	36,0	384	20	20	5,21E-08	4,40E-08		191	20,5	20,5	1,05E-03	998,18	38	-2,5	0,04	-0,13	0,02	0,06
Step06	215	-1,8	-1,8	334	-6	6,7	329	20	20	6,08E-08	5,13E-08		20,5	20,5	20,5	1,05E-03	998,18	40	-2,0	0,89	0,63	0,54	1,46
Step07	252	2,8	2,8	575	3	11,5	579	20	20	3,45E-08	2,91E-08		236	20,6	20,6	1,05E-03	998,16	33	7,0	0,40	0,43	0,38	0,42
Step08	275	1,6	1,6	384	-5	7,7	380	10	10	2,63E-08	2,22E-08		288	20,6	20,6	1,05E-03	998,16	31	2,9	0,55	0,53	0,51	0,61
Step09	306	1,2	1,2	501	-3	10,0	499	10	10	2,00E-08	1,69E-08		326	20,6	20,6	1,05E-03	998,16	28	2,7	0,45	0,47	0,41	0,50
Step10	335	0,2	0,2	471	2	9,4	474	10	10	2,11E-08	1,78E-08		345	20,6	20,6	1,05E-03	998,16	28	-0,5	-0,41	-0,35	-0,68	-0,27
Step11	348	-3,6	-3,6	48	0	1,0	49	2	2	4,12E-08	3,48E-08		346	20,7	20,7	1,04E-03	998,14	35	-7,1	0,51	0,51	0,49	0,54
Step12	364	3,1	3,1	95	-1	1,9	95	2	2	2,11E-08	1,78E-08		386	20,7	20,7	1,04E-03	998,14	28	7,1	0,44	0,44	0,42	0,46
Step13	379	1,2	1,2	120	-3	3,3	117	2	2	1,71E-08	1,44E-08		20,7	20,7	20,7	1,04E-03	998,14	26	1,9	0,63	0,58	0,55	0,73
Step14	397	1,6	1,6	181	2	3,6	183	2	2	1,09E-08	9,20E-09		20,7	20,7	20,7	1,04E-03	998,14	23	3,7	0,44	0,49	0,41	0,47
Step15	412	-0,4	-0,4	149	-1	3,0	148	2	2	1,35E-08	1,14E-08		20,7	20,7	20,7	1,04E-03	998,14	24	-1,7	0,24	0,27	0,21	0,27
Step16	425	-4,8	-4,8	57	-1	1,1	57	2	2	3,53E-08	2,98E-08		421	20,7	20,7	1,04E-03	998,14	34	-9,2	0,52	0,53	0,51	0,54
Step17	439	3,9	3,9	135	1	2,7	136	2	2	1,47E-08	1,24E-08		428	20,8	20,8	1,04E-03	998,12	25	8,6	0,46	0,47	0,44	0,47
Step18	454	2,1	2,1	215	-1	4,3	215	2	2	9,30E-09	7,85E-09		469	20,8	20,8	1,04E-03	998,12	22	3,5	0,59	0,59	0,56	0,63
Step19	472	0,7	0,7	291	1	5,8	292	2	2	6,84E-09	5,77E-09		20,8	20,8	20,8	1,04E-03	998,12	19	2,1	0,33	0,34	0,31	0,36
Step20	487	-0,4	-0,4	223	-20	20,4	203	2	2	9,85E-09	8,30E-09		20,8	20,8	20,8	1,04E-03	998,12	22	-2,5	0,16	0,22	0,13	0,21
Step21	516	-6,1	-6,1	61	-1	1,2	61	2	2	3,29E-08	2,78E-08		491	20,9	20,9	1,04E-03	998,10	33	-10,9	0,56	0,54	0,53	0,60

Notes: (a)The type of distribution associated with an assumption (green cell) is specified in the adjacent text as (N) for normal distribution and (U) for uniform. Standard deviation is specified in the cell closest on the right side, and is specified as a number or percent of the variable value. (b)The variability of each variable is achieved by adding the assumed distributions to the point value. For example $\Delta a_{adj.}$ is calculated as $\Delta a + N(0; (\Delta a * 0.02)^2) + N(0; (\Delta a * 0.01)^2)$.